

A new species of *Bathynomus* Milne-Edwards, 1879 (Isopoda: Cirolanidae) from the southern Gulf of Mexico with a redescription of *Bathynomus jamesi* Kou, Chen and Li, 2017 from off Pratas Island, Taiwan

Ming-Chih Huang, Tadashi Kawai & Niel L. Bruce

To cite this article: Ming-Chih Huang, Tadashi Kawai & Niel L. Bruce (2022) A new species of *Bathynomus* Milne-Edwards, 1879 (Isopoda: Cirolanidae) from the southern Gulf of Mexico with a redescription of *Bathynomus jamesi* Kou, Chen and Li, 2017 from off Pratas Island, Taiwan, *Journal of Natural History*, 56:13-16, 885-921, DOI: [10.1080/00222933.2022.2086835](https://doi.org/10.1080/00222933.2022.2086835)

To link to this article: <https://doi.org/10.1080/00222933.2022.2086835>



Published online: 09 Aug 2022.



Submit your article to this journal [↗](#)



View related articles [↗](#)



View Crossmark data [↗](#)



A new species of *Bathynomus* Milne-Edwards, 1879 (Isopoda: Cirolanidae) from the southern Gulf of Mexico with a redescription of *Bathynomus jamesi* Kou, Chen and Li, 2017 from off Pratas Island, Taiwan

Ming-Chih Huang ^a, Tadashi Kawai ^b and Niel L. Bruce ^{c,d}

^aDepartment of Biological Sciences and Technology, National University of Tainan, Tainan City, Taiwan, ROC;

^bCentral Fisheries Research Institution, Hokkaido Research Organization, Yoichi, Japan; ^cBiodiversity & Geosciences Program, Queensland Museum, South Brisbane, Australia; ^dWater Research Group, Unit for Environmental Sciences and Management, North-West University, Potchefstroom, South Africa

ABSTRACT

Bathynomus jamesi Kou, Chen and Li, 2017 from Zhengbin fishing port in Keelung, Taiwan, was identified by the shape of the distolateral corner of the uropodal endopod, the shape of the clypeus, and the nucleotide sequences of the COI (cytochrome *c* oxidase subunit 1) and 16S rRNA genes. Only two species of *Bathynomus* have previously been recorded from Taiwan, *B. doederleini* Ortmann, 1894 and *B. decemspinus* Shih, 1972. *Bathynomus kensleyi*, previously known from the South China Sea as well as the south-east Swain Reefs, Coral Sea, was primarily differentiated by the elongate and upturned pleotelson spines, but that character is now shown to also occur in mature *Bathynomus jamesi*. Two specimens from the Gulf of Mexico (obtained from the Enoshima Aquarium in Japan) were compared to species of *Bathynomus* from the western North Atlantic. Sequence data showed that one of two samples was not *B. giganteus* Milne-Edwards, 1879, as had been assumed, and it did not match any other species of *Bathynomus*. That specimen was collected off the Yucatán Peninsula and is morphologically distinct from both *B. giganteus* (in the relative length of the antennal flagellum and the length:width ratio of the pleotelson) and *B. maxeyorum* Shipley, Brooks, and Bruce in Shipley et al., 2016 (the number of pleotelson spines is seven and the distolateral corner is produced on the uropodal exopod). Therefore, it is here described as *B. yucatanensis* sp. nov. *Bathynomus* is currently a very minor fisheries resource in Taiwan and Japan, but this find demonstrates the continuing importance of the fishing industry to marine biological exploration.

<http://www.zoobank.org/urn:lsid:zoobank.org:pub:399605D3-356E-402D-9ED1-E36A649A3F1B>

ARTICLE HISTORY

Received 20 February 2022

Accepted 24 May 2022

KEYWORDS

Cirolanidae; South China Sea; Taiwan; *Bathynomus kensleyi*; *Bathynomus yucatanensis* sp. nov

Introduction

The scavenging genus *Bathynomus* (Milne-Edwards, 1879) is common in the tropical and temperate deep sea (Milne-Edwards 1879; Milne-Edwards and Bouvier 1902; Holthuis and Mikulka 1972). Nineteen extant and four fossil species have been described (Sidabalok

CONTACT Ming-Chih Huang mingchih39@mail.nutn.edu.tw

© 2022 Informa UK Limited, trading as Taylor & Francis Group

et al. 2020). The most recent comprehensive account of the genus is that of Lowry and Dempsey (2006), who recognised two distinct morphological groups within the genus that they termed ‘giants’ and ‘super-giants’. Both groups are found in the Atlantic and Indo-West Pacific regions, from 35°N to 35°S and at 70–2500 m depth (Lowry and Dempsey 2006). A further three species have been described since 2016: *Bathynomus jamesi* Kou, Chen and Li, 2017, *Bathynomus maxeyorum* Shipley, Brooks and Bruce, 2016 and *Bathynomus raksasa* Sidabalok, Wong and Ng, 2020.

In the 1970s, a deep seabed trawl fishery emerged in Taiwan. Fishermen in what is now the Ruifang District of New Taipei City on Taiwan’s north-eastern coast began to eat *Bathynomus*, prepared by steaming them like lobsters or crabs and calling them ‘Tua Hay-Shi’ (‘big sea lice’ in Taiwanese). Soong (1992) identified the species as *B. giganteus* Milne-Edwards, 1879, a species that is now known to be restricted to the tropical western Atlantic (Magalhães and Young 2003; Lowry and Dempsey 2006). Two species are definitively known from Taiwan: *B. doederleini* Ortmann, 1894 from off Taitung in eastern Taiwan (Soong and Mok 1994) and *B. decemspinus* Shih, 1972 from the Taiwan Strait west of Tungkang (= Donggang) port in southern Taiwan (Shih 1972).

In this paper, we originally wanted to explore the species identity and morphological characteristics of 10 *Bathynomus* individuals taken from the Pratas Islands. In order to facilitate the study two *Bathynomus* specimens were obtained from an aquarium in Japan for comparison, one species was *B. giganteus* and the other proved to be an undescribed species. Using molecular biology methods to analyse cytochrome *c* oxidase I (COI) and 16S rRNA sequences, we confirmed the relationship between individuals.

Comparative material from the Gulf of Mexico proved not to belong to *B. giganteus*. We therefore take this opportunity to propose a new western North Atlantic species of *Bathynomus* and provide a name, diagnosis, description, and illustrations.

Materials and methods

Specimen collection

Several specimens (TMCD003326–003330, EA0238, Table 1) were purchased at the Zhengbin fishing port in Keelung, Taiwan, captured in waters around Pratas Island about 450 km south-west of Kaohsiung, Taiwan (Figure 1). The other specimens (TMCD003331–003334, Table 1) were captured in waters of the South China Sea about 300 km south-west of Pratas Island. Pratas Island (Dongsha Island in Mandarin), is the only island on a large atoll. The Dongsha Marine National Park was established on account of the well-conserved marine ecosystem there. The present specimens were taken from waters outside the protected area, preserved on ice aboard ship, and then stored at –20°C in the laboratory. This allowed us to observe the fresh body colour. For comparative purposes, we used the exchange method to obtain two *B. giganteus*, and sent two *B. jamesi* to the Enoshima Aquarium (Fujisawa, Kanagawa, Japan). According to the aquarium records, they were caught in a baited cage at a depth of 600–800 m on 19 April 2017 in the Gulf of Mexico off the Yucatán Peninsula.

Ten specimens of *Bathynomus jamesi* were obtained from Pratas Island and the South China Sea, and two *Bathynomus* including the holotype of *D. yucatanensis* sp. nov. and *B. giganteus* (Table 1) have been deposited and registered in the National Taiwan

Table 1. Intraspecific variation of morphology of *Bathynomus jamesi*, *B. giganteus* and *B. yucatanensis* sp. nov.

TMCD00	Species	Locality	Sex	TL (mm)	CL (mm)	Weight (g)	Spike num	Body type	Maximum width	Antenna 2 flagellum extending to	Pleotelson length-width ratio	Shape of pleotelson spines	Ana. Gene	NCBI No. (COI, 16S)	Fig
3326	<i>B. jamesi</i>	Pratas	Female	309	150	1100	13	Slender	Pereonite 4	Pereonite 2	1.62	Upwardly curved	COI	MW575424	9, 11
3327	<i>B. jamesi</i>	Pratas	Male	355	197	2000	13	Stout	Pereonite 5	Pereonite 2	2.71	Upwardly curved	COI	MW575449	11
3328	<i>B. jamesi</i>	Pratas	Male	321	169	1525	13	Stout	Pereonite 5	Pereonite 3	2.63	Upwardly curved	COI	MW575455	8, 11
3329	<i>B. jamesi</i>	Pratas	Female	318	147	1100	11	Stout	Pereonite 5	Pereonite 2	2.45	Upwardly curved	COI, 16S	MW580729, MZ029589	9, 11
EA0238*	<i>B. jamesi</i>	Pratas	Male	313	164	1175	13	Stout	Pereonite 5	Pereonite 2	1.96	Upwardly curved	COI	MW580730	11
3330	<i>B. jamesi</i>	Pratas	Male	376	169	1510	11	Stout	Pereonite 5	Pereonite 2	1.51	Upwardly curved	COI	MW575454	11
3331	<i>B. jamesi</i>	Pratas	Female	298	117	600	13	Stout	Pereonite 5	Pereonite 2	1.56	Upwardly curved	COI	MW577650	11
3332	<i>B. jamesi</i>	Pratas	Female	277	115	495	11	Stout	Pereonite 5	Pereonite 2	1.71	Upwardly curved	COI	MW577651	3, 11
3333	<i>B. jamesi</i>	Pratas	Male	309	150	1125	13	Stout	Pereonite 5	Pereonite 3	2.09	Upwardly curved	COI	MW579548	11
3334	<i>B. jamesi</i>	Pratas	Male	356	173	1600	13	Slender	Pereonite 4	Pereonite 2	1.97	Upwardly curved	COI	MW577652	11
Holotype**	<i>B. jamesi</i>	Hainan	Female	114	N/A	N/A	13	N/A	N/A	Pereonite 3	1.33	Straight	COI, 16S	KX417647, KX417643	11, 20
3335	<i>B. yucatanensis</i>	Yucatán	Male	260	129	550	12	Slender	Pereonite 5	Pereonite 3	2.08	Straight	COI, 16S	MZ354630, MZ042927	19, 20
3336	<i>B. giganteus</i>	Yucatán	Male	316	172	856	13	Stout	Pereonite 5	Pereonite 2	2.12	Straight	COI, 16S	MG229639, MG229479	19, 20

*EA0238 stored in Enoshima Aquarium, Japan. **Holotype, data from Kou et al. (2017). Ana: analyze, CL: cephalic length, COI: cytochrome oxidase I, Fig: figure, Num: number, TL: total length.

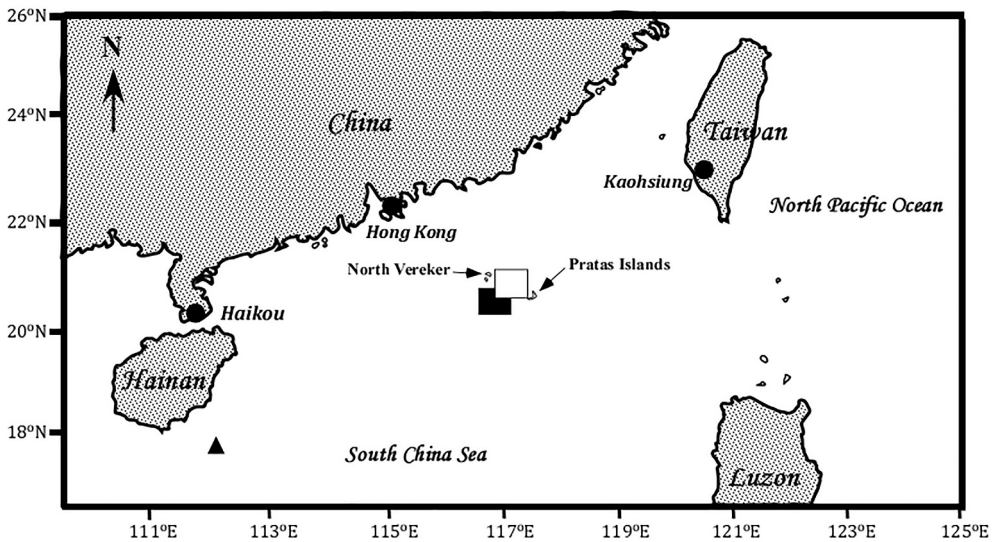


Figure 1. Map of Taiwan, Pratas Island and Hainan. The sampling site of *Bathynomus kensleyi* of Lowry and Dempsey (2006) is between North Vereker bank and Pratas Island, indicated by an open square (□), and the *Bathynomus kensleyi* of Lowry and Dempsey (2006) sampling site is indicated by a black square (■) (Lowry and Dempsey 2006). The black triangle (▲) indicates the sampling site of *Bathynomus jamesi* from Kou et al. 2017.

Museum, Taipei (registration code: Taiwan Museum code, TMCD, from TMCD003326 to TMCD003336). Two *B. jamesi* were donated to Enoshima Aquarium, Japan, namely EA0238 and EA0243 (the latter was not included among the 10 analysed samples).

Abbreviations. AM – Australian Museum, Sydney; CL – cephalic length; COI – cytochrome c oxidase subunit 1; NMMB – National Marine Biology Museum, Taiwan; NMHN – Muséum National d’Histoire Naturelle, Paris; QM – Queensland Museum, Brisbane; RS – robust seta/e; TL – total length; TMCD – National Taiwan Museum code.

Morphological observations

The whole specimen and dissected body parts (voucher numbers: TMCD003332 and TMCD003335) were photographed using a high-resolution monocular camera (Canon EOS 90D, Tokyo, Japan). Line drawings were produced by tracing ink-jet-printed digital images in black ink on a light table. These drawings were digitally scanned and then assembled into plates using Adobe Illustrator CS (Adobe Inc., San Jose, CA, USA). The terminology of body parts follows Kensley and Schotte (1989), Keable (2006), Lowry and Dempsey (2006), and Bruce (2009). Total length (TL) and cephalic length (CL) were measured from the anterior tip to posterior end, respectively.

Molecular biological analysis

Total genomic DNA was extracted from ca. 25 mg each of pereopod muscle resected from all 10 specimens from off Pratas Island waters and both specimens from off the Yucatán Peninsula, using a commercial genomic DNA extraction kit (QIAamp DNA Mini Kit, Hilden,

Germany) according to the manufacturer's protocol. Polymerase chain reaction (PCR) primers used for the amplification were designed based on the sequences of the genes encoding COI (Folmer et al. 1994) and 16S ribosomal RNA (Palumbi et al. 1991) of *B. jamesi* and *B. yucatanensis*. In addition, using the COI sequence confirms primers as test of COI (TESCOI) for double-checking (Table 2). All samples were sequenced for COI (10 of *B. jamesi*, one of *B. giganteus*, and one of *B. yucatanensis*), and two individuals were sequenced for 16S rRNA (TMCD003329 and TMCD003335) (Table 1).

Amplification using the COI and 16S rRNA primers was based on a cycle of denaturation at 94°C for 30s, annealing at 48°C for 40s, and extension at 72°C for 30s using a DNA thermal cycler model MyCycler™ Thermal Cycler System (#1709703, Bio-Rad, Hercules, CA, USA). This procedure was carried out for 35 cycles, and the final extension step was performed at 72°C for 10 min. The 100 µL reaction medium contained 200 nM dNTPs, 10 mM each of forward and reverse primers, 2 units of Ex Taq DNA polymerase (TaKaRa Ex Taq® DNA Polymerase, Takara Bio, Shiga, Japan), 10 µL of 2× Ex-Taq DNA polymerase buffer (Takara Bio), and 50 ng of genomic DNA. The PCR products were subjected to electrophoresis using 1% agar (VWR Funding Inc, West Chester, PA, USA) and visualised with SYBR Green (HealthView Nucleic Acid Stain, Thermo Fisher Scientific, Waltham, MA, USA). After confirming the success of PCR amplification, the products were sent to Biotech (Genomics, Xizhi District, New Taipei City, Taiwan) for sequencing. The obtained sequences were edited and aligned using BioEdit 7.2 editing software (<https://www.mybiosoftware.com/bioedit-7-0-9-bio-logical-sequence-alignment-editor.html>) and Multiple Sequence Alignment (Clustal Omega – GenomeNet, Hinxton, Cambridgeshire, UK).

Molecular systematics analysis

Comparisons of the edited and aligned COI and/or 16S rRNA sequences of the present specimens and five previously sequenced species of *Bathynomus* were performed using Molecular Evolutionary Genetics Analysis 11 (MEGA 11) software (Tamura et al. 2021). COI sequence data were obtained from the National Center for Biotechnical Information (NCBI) for *B. giganteus* (MG229639) (from the northern Gulf of Mexico, with the exception of De Soto Canyon; Timm et al. 2018), *B. jamesi* (KX417647) (from the sea off the southern part of Hainan Island, China; Kou et al. 2017), *B. maxeyorum* (KT963292) (from north-east

Table 2. List of primer pairs and PCR annealing temperatures (T_m) used to amplify COI and 16S rRNA genes.

Primers	Sequence 5'–3'	T_m (°C)
COI primers (Folmer et al. 1994):		
LCO-1490 (F)	GGT CAA CAA ATC ATA AAG ATA TTG G	48
HCO-2198 (R)	TAA ACT TCA GGG TGA CCA AAA AAT CA	48
TESCOI (F)	TAG TGG TAA CGG CTC ATC CC	53
TESCOI (R)	GCA TTG TAA TAG CTC CCG CC	53
16S primers (Palumbi et al. 1991):		
16Sar (F)	CGC CTG TTT ATC AAA AAC AT	56
16Sbr (R)	CCG GTC TGA ACT CAG ATC ACG T	56

Exuma Sound, Western Atlantic Ocean; Shipley et al. 2016), *B. doederleini* (MZ723938) (from Sagami Bay, Japan; unpublished). 16S rRNA sequences were obtained for *B. jamesi* (KX417643) (from the sea off the southern part of Hainan Island, China, Kou et al. 2017) and *B. giganteus* (MG229479) (from the northern Gulf of Mexico, with the exception of De Soto Canyon, Timm et al. 2018).

The nucleotide sequence for Cirolanidae (*Atarbolana exoconta* Bruce and Javed, 1987) COI (KX782999) was used as the outgroup control. Using Drawtree (Phylip software package, <http://bioweb.pasteur.fr/seqanal/interfaces/drawtree.html>), phylogenetic trees were constructed by the neighbour-joining (NJ) method under a number of different methods (Nei and Kummer 2000).

Results

Order Isopoda Latreille, 1817

Family Cirolanidae Dana, 1852

Genus *Bathynomus* Milne-Edwards (1879)

***Bathynomus jamesi* Kou, Chen and Li, 2017**

Bathynomus giganteus – Soong 1992: 293, figs 1, 2 [not *Bathynomus giganteus* Milne Edwards, 1879].

Bathynomus kensleyi – Lowry and Dempsey 2006: 184 [South China Sea and Philippine specimens only].

Bathynomus kenleyi – Truong 2015: 81, fig. 2 [lapsus].

Bathynomus jamesi Kou, Chen and Li, in Kou et al. 2017: 285, figs 2–7.

Material examined

Four ovigerous females, Pratas Island voucher numbers TMCD003326, 3329, 3331 and 3332, TL 277–318 mm (avg. 300.5 mm), CL 115–150 mm (avg. 132.3 mm), wet weight 495–1100 g (avg. 823.8 g). Six males (TMCD003327, 003328, 003330, 003333, 003334 and EA0238), TL 309–376 mm (avg. 338.3 mm), CL 150–197 mm (avg. 170.3 mm), wet weight 1125–2000 g (avg. 1489.2 g) (Table 1). Males are slightly larger than females. Six specimens (TMCD003326–3330 and EA0238) were collected by bottom trawl in the northern South China Sea between North Vereker Bank (21.061°N, 116.109°E) and Pratas Island (20.717°N, 116.700°E) by the crew of the Keelung-based fishing vessel *Jin Ruiyi 37* on 17 June 2019 (Figure 1), and four specimens (TMCD003331–3334) were collected by bottom trawl about 300 km south-west of Pratas Island (19.084°N, 115.250°E) by the crew of the Keelung-based fishing vessel *Jing yang* on 12 May 2020. The water depth was about 420–550 m.

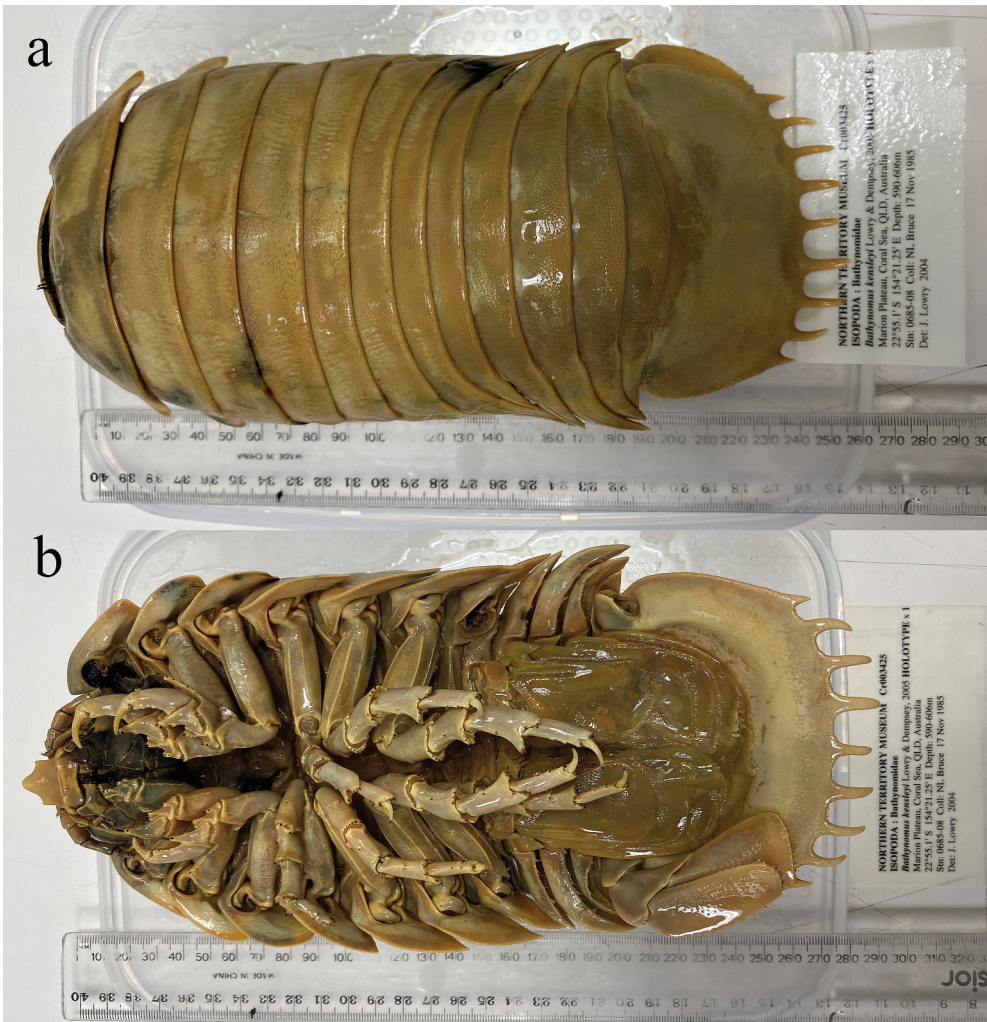


Figure 2. Holotype of *Bathynomus kensleyi*. (a) Dorsal view; (b) ventral view (voucher number: Northern Territory Museum Cr003425), Marion Plateau, Coral Sea, QLD, Australia (22.918°S, 154.354° E, depth, 590–606 m, Stn:0685–08, coll: NL Bruce, 17 November 1985, det: J. Lowry 2004). (Photo provided by Gavin Dally, Senior Collections Manager Natural Sciences, Northern Territory Museum, Australia).

Also examined. Photographs of *Bathynomus kensleyi* holotype (NTM Cr003425) (Figure 2). Marion Plateau, Coral Sea, QLD, Australia (22.917°S, 154.350°E, depth, 590–606 m, Stn: 0685–08, coll: N.L. Bruce, 17 November 1985, det: J. Lowry 2004) (Photo provided by Gavin Dally, Senior Collections Manager Natural Sciences, Northern Territory Museum), Australia). Imm, 129 mm, off Lihou Reef, Coral Sea, 16.917°S, 155.567°E, 6 October 1985, 880 m, coll. RV *Soela* (QM W28011). Photographed material identified as *Bathynomus kensleyi* by Lowry and Dempsey

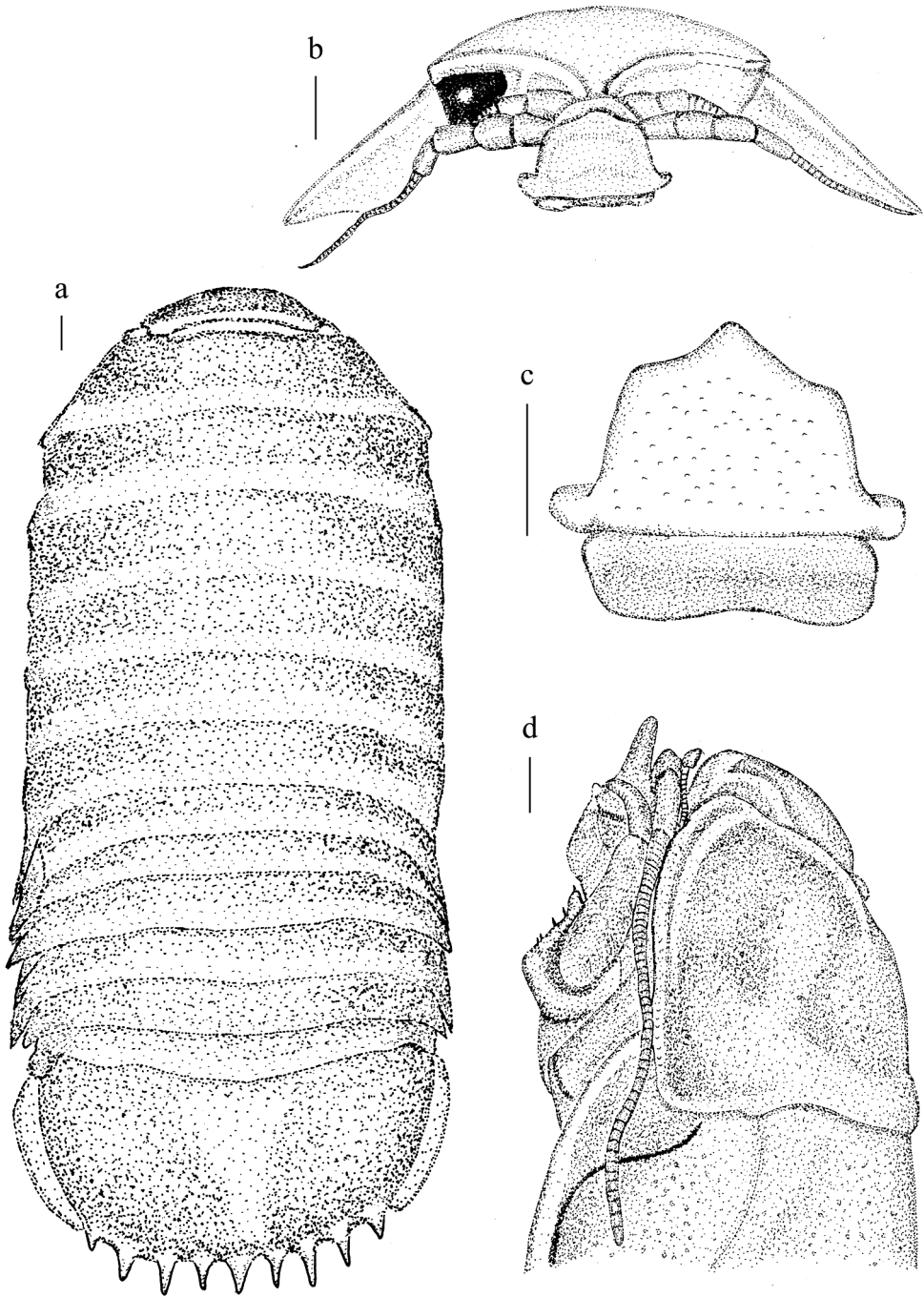


Figure 3. *Bathynomus jamesi* (voucher no. TMCD003332). (a) Body, dorsal view; (b) cephalon, anterior view; (c) clypeal region, ventral view; (d) cephalon, lateral view. Scale bars: 1 cm.

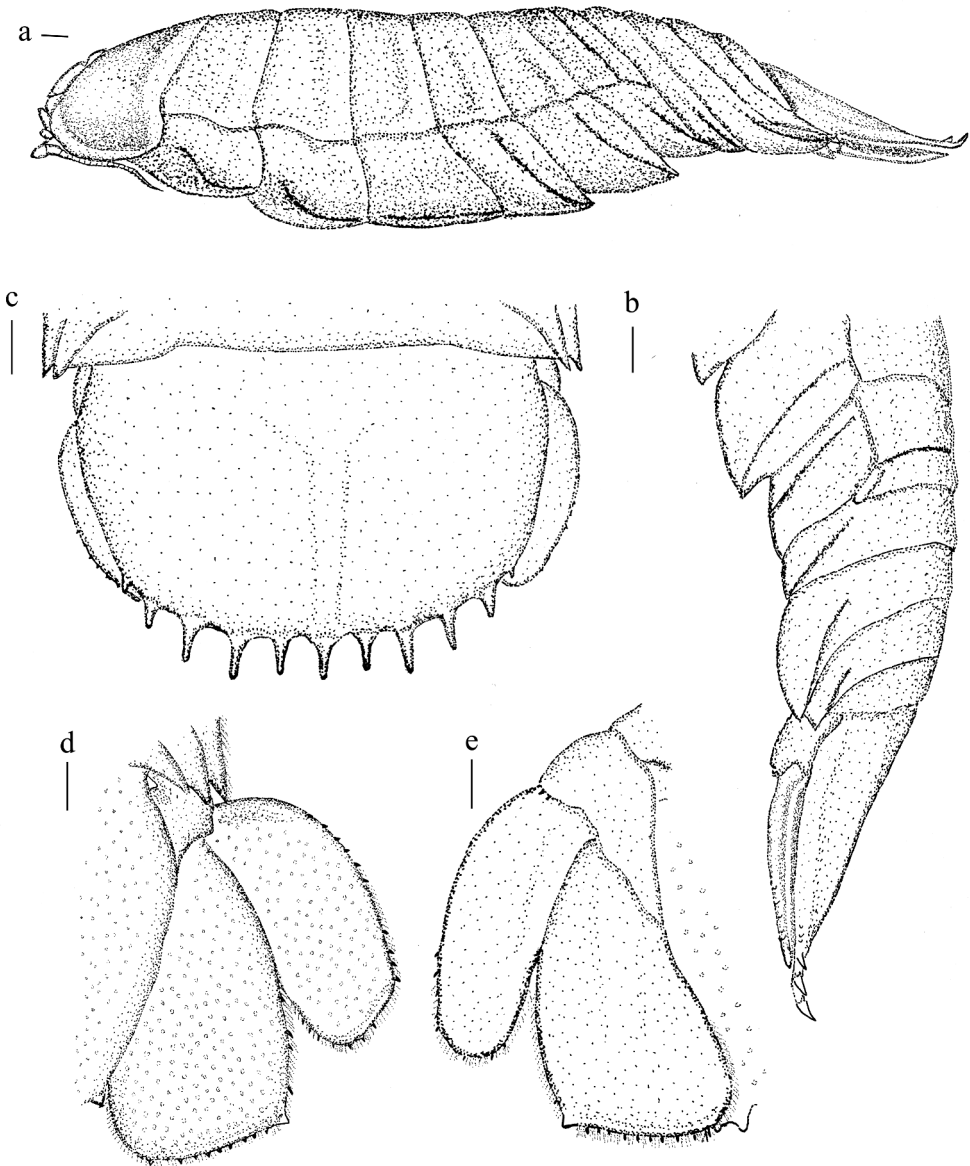


Figure 4. *Bathynomus jamesi* (voucher no. TMCD003332). (a) Body lateral view; (b) pereion lateral view; (c) pleotelson, dorsal view; (d) uropod dorsal view; (e) uropod ventral view. Scale bars: 1 cm.

(2006): from Sulu Sea (AM P42711, P42712), south of Hong Kong [Soong (1992) material, NMMB-CD005878, Taiwan], and material from off Lubang Island, near Manila, Philippines, MNHN IS.2290, IS.2298).

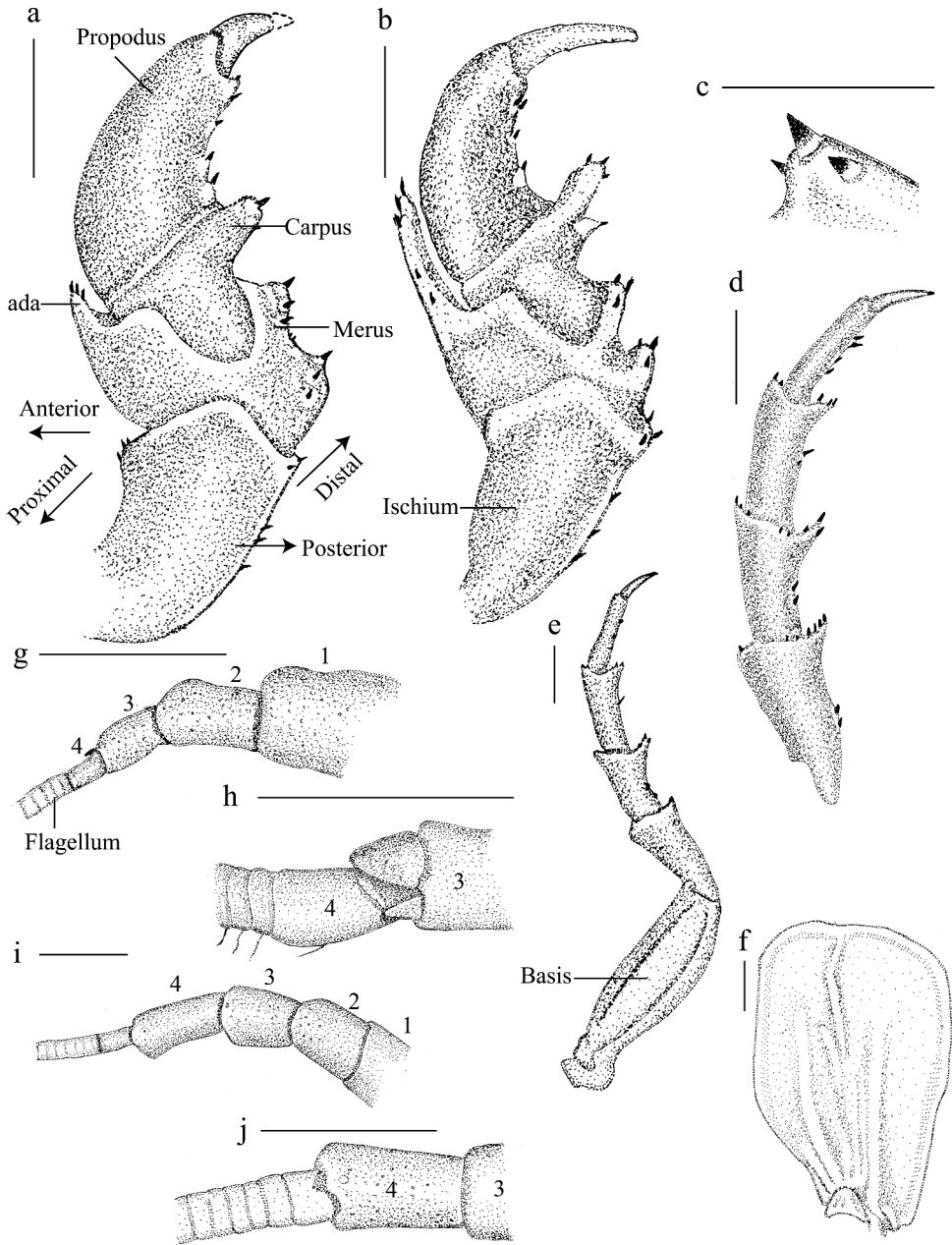


Figure 5. *Bathynomus jamesi* (voucher no. TMCD003332). (a) Pereopod 1, mesial view; (b) pereopod 2, mesial view; (c) pereopod 2 merus, posterolateral margin, (d, e) pereopod 7; (f) oostegite of pereopod 2; (g) antenna; (h) region of antennal peduncle articles; (i) antennal peduncle; (j) region of antennal peduncle articles. ada, anterodistal angle. Scale bars: 1 cm.

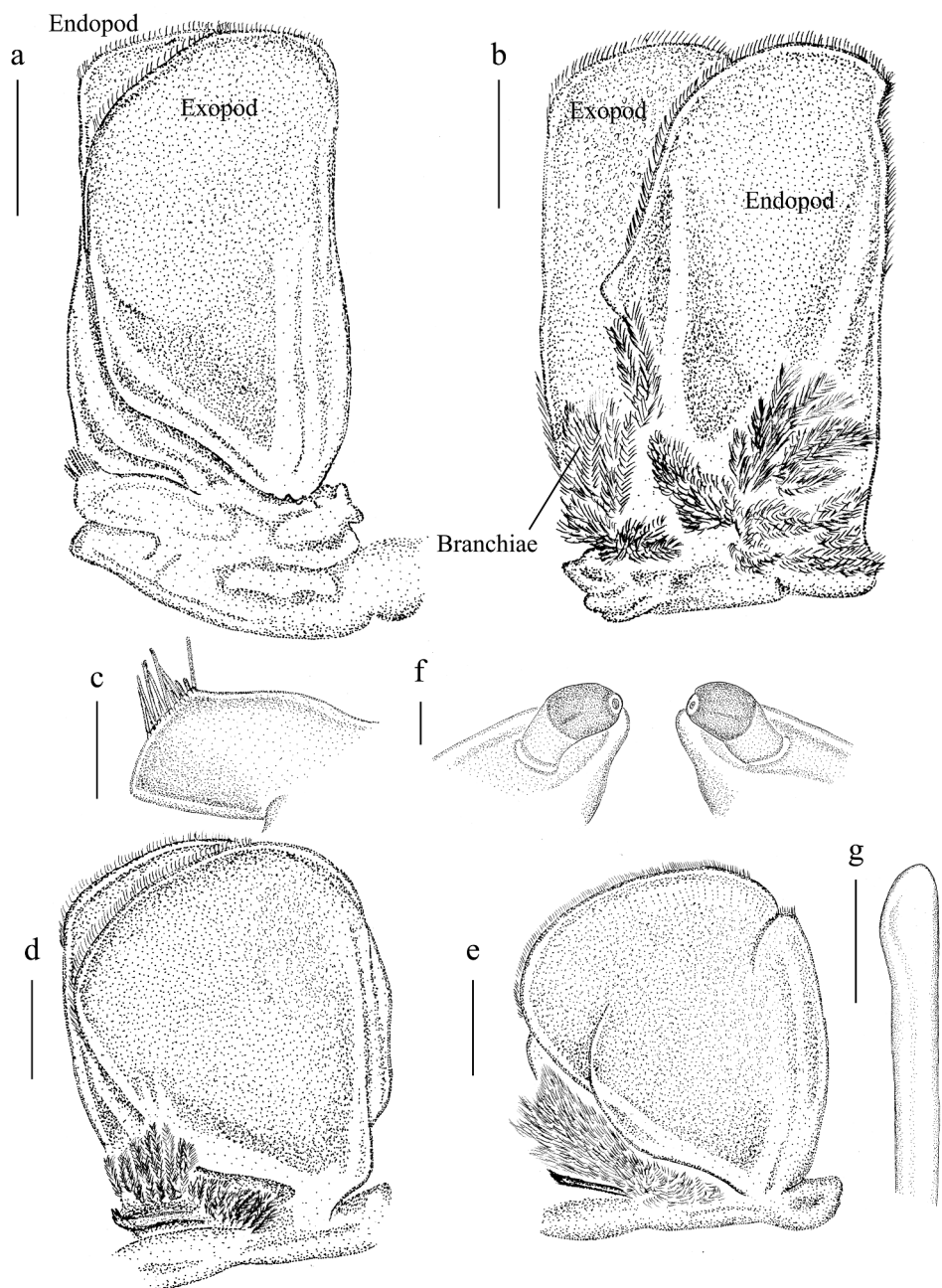


Figure 6. *Bathynomus jamesi* (voucher no. TMCD003332 female for (a–e), TMCD003327 male for (f–g)). (a) Pleopod 1, ventral view; (b) pleopod 1, dorsal view; (c) peduncle, ventral view; (d) pleopod 2, ventral view; (e) pleopod 3, ventral view; (f) penes; (g) apex of appendix masculina. Scale bars: a, b, d–g = 1 cm; c = 0.5 cm.

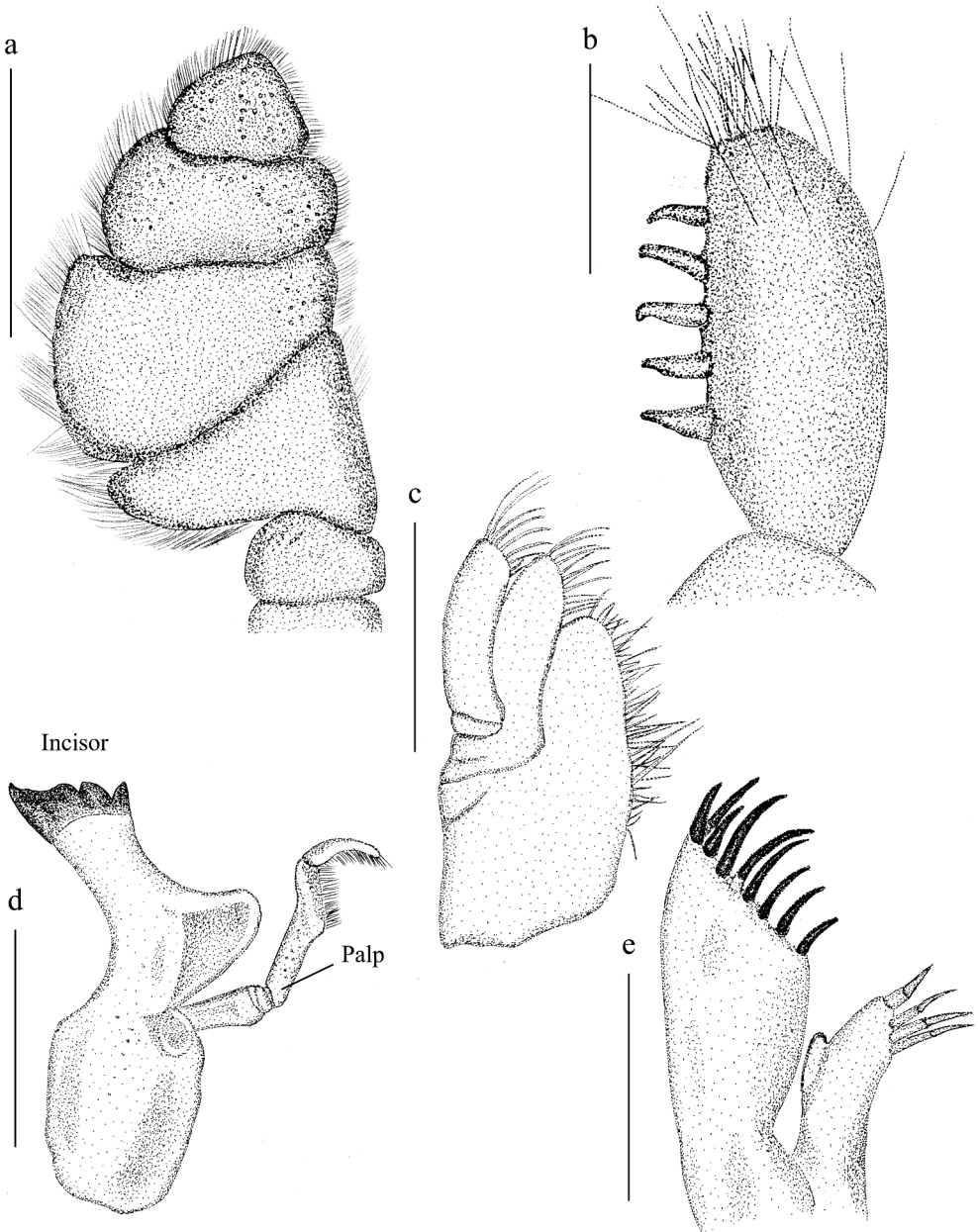


Figure 7. *Bathynomus jamesi* (voucher no. TMCD003332) mouth parts. (a) Maxilliped palp; (b) maxilliped endite; (c) maxilla; (d) mandible; (e) lateral lobe of maxilla. Scale bars: 1 cm.

Description of a female (TMCD003332)

Body 2.4 times as long as wide, ovate in shape, coarsely punctate, without sculpture (Figure 3(a)); 277 mm in TL. Head ridge above eyes discontinuous (Figure 3(b)). Clypeal region distal margin slightly concave, apex narrowly rounded (Figure 3(b,c)).

Antennula peduncle 4-articulate (Figure 5(g)) with 4 articles with exopod at end of peduncular article 4 (Figure 5(h)); flagellum longer than peduncle. Antenna peduncle article 4 very short (Figure 5(i)), article 4 about 2.5 times longer than article 3, articles 1–2 bearing neither exopod nor seta (Figure 5(i)), composed of approximately 50 articles; flagellum longer than peduncle, extending to within pereonite 2 (Figures 3 (d) and 4(a)), composed of approximately 60 articles (near-terminal segmentation unclear).

Palp not reaching to incisor margin (Figure 7(d)). Maxilla with long setae (Figure 7 (c)); lateral lobe with 9 keratinised spines on exopod, 4 robust spines on endopod (Figure 7(e)). Maxillipedal endite with 5 equally spaced, robust, spiniform setae (Figure 7(b)).

Pereopod 1 (Figure 5(a)) ischium bearing 3 posteroproximal RS and 3 RS on posterodistal margin; merus with 3 RS on an anterodistal angle, proximal row of 3 RS on posterolateral margin, and distal row of 3 RS; propodus twice as long as wide, with 4 RS on posterior margin. Pereopod 2 (Figure 5(b)) ischium with 3 RS each on posterior and posterodistal margins; merus with 5 short simple setae on an anterodistal angle, 3 RS in a proximal row on posteromedial margin, and distal row of 3 RS; propodus with 4 RS on posterior margin. Pereopod 7 basis 2.5 times as long as greatest width, superior margin convex, inferior margin with 5 palmate setae; ischium 0.7 times as long as basis, inferior margin with 14 RS (4 clusters of 1 + 3 + 6 + 4), superior distal angle with 12 RS, inferior distal angle with 6 RS; merus 0.5 as long as ischium, 2.1 times as long as wide, inferior margin with 6 RS, superior distal angle with 9 RS, inferior distal angle with 8 RS; carpus 0.6 as long as ischium, 1.6 times as long as wide, inferior margin with 5 RS (as 1 + 2), superior distal angle with 13 RS, inferior distal angle with 9 RS; propodus 0.7 as long as ischium, 2.4 times as long as wide, inferior margin with 6 clusters of RS (as 3 clusters of 2), superior distal angle with 4 slender setae, inferior distal angle with 1 RS; dactylus 0.5 as long as propodus.

Oostegites arise from proximal parts of pereopods 1–6 (Figure 5(f)). Coxa of pereopod 7 distally broadened and slightly curved posteriorly (Figures 4(a,b)).

Pleon comprising approximately 20% of body length (Figures 3(a) and 4(a)). Posterolateral angles of pleonites 3–4 reaching to almost the same level posteriorly (Figure 4(a,b)). Apex of appendix masculina simple and flat (Figure 6(g)). Penial processes close-set, 0.86 times as long as basal width, distally bluntly rounded (Figure 6(f)).

Pleotelson (Figure 4(b,c)) 0.6 times as long as greatest width, smooth except for minute pores, with inconspicuous longitudinal carina on dorsal surface; posterior margin with 11 long, prominent, upwardly curved spines and pair of small posterolateral spines, without setae between spines, central spine simple.

Uropods (Figure 4(c)) not extending beyond caudal margin of pleotelson. Peduncle with 2 RS on caudolateral margin (Figure 4(e)). Exopods and endopods both with continuous marginal setal fringes and smooth lateral and distal margins (Figure 4(d)). Lateral margin of exopod convex with 9 RS, setal fringe continuous 75% (Figure 4(d)), medial margin straight, distomesial corner rounded, and distal margin convex with 4 RS, distolateral corner slightly produced, subacute. Endopod with subacute distolateral angle, straight lateral margin with 3 RS, straight medial margin, rounded distomesial corner, and straight distal margin with 10 RS, distolateral corner produced, subacute.



Figure 8. *Bathynomus jamesi* (voucher no. TMCD003328), body length 321 mm. (a) Dorsal view; (b) ventral view. Each square is 10 mm on a side.

Colour of dorsal surfaces dark yellowish-grey; pleotelson light grey; ventral sides of pereopods, pleotelson, and uropods also light grey, but pleopods dark rose (Figure 8(b)).

Habitat

Continental slope, bathyal to the upper abyss (300–2500 m) (Lowry and Dempsey 2006),

Distribution

South China Sea off Hainan Island, south-east of Hong Kong, off Taiwan and off western Luzon Island, Philippines; continental slope at depths between 300 and 925 metres (Lowry and Dempsey 2006).

Variation. Specimens TMCD003326–3334, and EA0238: variation appears in body length/width ratio (1.80–2.55), flagellum length (extending to within pereonite 2 and/or 3), pleotelsonic length/width ratio (1.51–2.71) and number of pleotelsonic spines (11 or 13). The smallest body length/width ratio is that of TMCD003327 (1.80), and TMCD003331 has the largest (2.55). Length of most flagella length extending to within pereonite 2 but TMCD003328 and TMCD003333 can extend to within pereonite 3. The pleotelsonic length/width ratio is also very different, with TMCD003330 being the smallest at 1.51, and TMCD003327 being the largest at 2.71. For most specimens the number of pleotelsonic spines is 13, but TMCD003329 and TMCD003330 have 11 (Table 1).

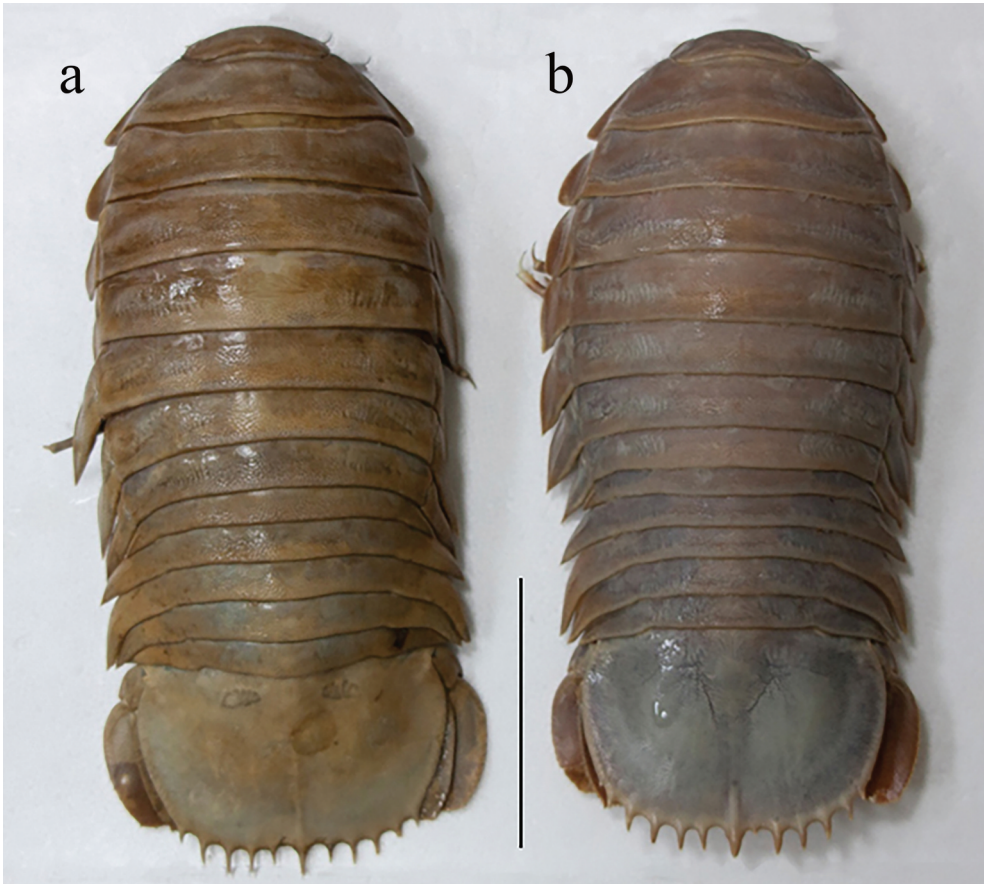


Figure 9. Two types of *Bathynomus jamesi*: slender (right, TMCD003329) and stout (left, TMCD003326). Scale bars: 10 cm.

Molecular biology. Amplified PCR products of 497 bp from 16S rRNA and 657 bp from COI, respectively, were obtained for the 16S rRNA and COI nucleotide sequences of one (TMCD003329) and nine (TMCD003326–003333) of our specimens *B. jamesi* (Table 1), respectively. The results of COI alignment showed that samples collected from Pratas Island are the same species as *B. jamesi* (Figures 10 and 11). The sequence data have been uploaded to the DNA Data Bank of Japan (DDBJ)/European Molecular Biology Laboratory (EMBL)/GenBank (Acc. Nos. MW575424, MW575449, MW575454, MW575455, MW580729, and MW580730 for COI, and MZ029589 for 16S rRNA). The variation in the 657-bp COI gene sequences cloned from individual *Bathynomus* involved 7 positions, with the less prevalent base-pairing usually occurring in just 1 or 2 specimens: c. 90T>C (MW577651), c. 255T>C (MW575454), c. 302T>C (MW575424), c. 498 A>G (MW575424), c. 558G>T (MW575454), and c. 573C>T (MW575449). The greatest number and variety of mutations were found at position 348: c. 348 A>T (MW575455), (MW580729), (MW580730), and c. 348 A>C (MW577651), (MW577652) (Figure 11).

After COI and 16S rRNA sequencing, and comparison with the NCBI databank, the results confirmed that the 10 specimens were all *B. jamesi* (Figure 11). The immature and juvenile specimens do not necessarily exhibit all the species characteristics found in fully adult specimens; in particular, the form of the pleotelson spines may be substantially different. So, new species should never be based on sub-adults (of any stage) where related species are very similar.

Remarks

Bathynomus jamesi was described from Hainan Island in the northern South China Sea (Kou et al. 2017). The diagnosis was ‘pleotelson with 11 or 13 short, straight spines; central spine not bifid. Uropod with endopod and exopod distolateral corner slightly produced. Clypeus lateral margins concave, narrowly rounded apically. Antennal flagellum extending to within pereonite 3’. Kou et al. (2017) did not describe any upward curvature of the pleotelsonic spines in their specimens from Hainan Island, something that is obvious in all 10 of our specimens. Another difference is the shorter antennal flagellum in our material, extending to pereonite 2 (a few to pereonite 3, see Table 1) but in the holotype and the original description by Kou et al. (2017) it is described as extending to pereonite 3.



Figure 10. Alignment of partial DNA sequence of the cytochrome c oxidase I from the South China Sea *Bathynomus* spp. They are *B. jamesi* (NCBI Acc. No. MW575454), *B. jamesi* (KX417647) and *B. doederleini* (MZ723938).

KX417647	TTTGGGGCTTGAGCGGGGCTGTTGCCACTGGSTGAGATAAATATOCGGTAGAGTITAGGSCAACCTGGCAGCTTTATTGGAGATGATCAGATCTATAATGATGGTAAACGGCGCAT	120
MW575424(1)	120
MW575449(2)	120
MW575455(3)	120
MW580729(4)	120
MW580730(5)	120
MW575454(6)	120
MW577650(7)	120
MW577651(8)C.....	120
MW579548(9)	120
MW577652(10)	120
KX417647	GCCITGTGTATGATTTTTTTTCTTGTTAACCGGTGATATTTGGGGATTTGGTAATTTGGCTTCTCCACTTATAATGGGGGGCCAGATATAGCAATTTCTCGGATAAATAATATAGA	240
MW575424(1)	240
MW575449(2)	240
MW575455(3)	240
MW580729(4)	240
MW580730(5)	240
MW575454(6)	240
MW577650(7)	240
MW577651(8)	240
MW579548(9)	240
MW577652(10)	240
KX417647	TTTIGACCTTACCTCCACTTTIAGCTCTCTTGTGAGGAGGGCTAGTAGAGGGGGTGGGACCGGCTGAACCGCTACCGCGGTTAGCAAGGGGTAITGCACATAGTGGGCT	360
MW575424(1)C.....	360
MW575449(2)	360
MW575455(3)T.....	360
MW580729(4)T.....	360
MW580730(5)T.....	360
MW575454(6)C.....	360
MW577650(7)	360
MW577651(8)C.....	360
MW579548(9)	360
MW577652(10)C.....	360
KX417647	TCGGTGAITTGCTAATTTTTTCTTTCATTIAGCAGGGGCTTCTCTATCTTAGGGCCAGTAAATTTTATGTCACCCCAATTAATATGCGCTCTTACGGGATAAGCCTGATCGATT	480
MW575424(1)	480
MW575449(2)	480
MW575455(3)	480
MW580729(4)	480
MW580730(5)	480
MW575454(6)	480
MW577650(7)	480
MW577651(8)	480
MW579548(9)	480
MW577652(10)	480
KX417647	CCACTTTTGTGGTCAAGTATTATACAGCGTACTATGCTGCTCTCTTCCAGTACTGGCGGGGCTATACAGATGCTTTTACAGATCGTAACTTAACTAGATCTTTTGAC	600
MW575424(1)G.....	600
MW575449(2)C.....	600
MW575455(3)C.....	600
MW580729(4)C.....	600
MW580730(5)C.....	600
MW575454(6)T.....C.....	600
MW577650(7)C.....	600
MW577651(8)C.....	600
MW579548(9)C.....	600
MW577652(10)C.....	600
KX417647	CCTAGAGGGGAGGAGACCTTATCTTACCAACACCTAATTTGATTTTTTGGT	654
MW575424(1)C.C.C	657
MW575449(2)C.C.C	657
MW575455(3)C.C.C	657
MW580729(4)C.C.C	657
MW580730(5)C.C.C	657
MW575454(6)C.C.C	657
MW577650(7)C.C.C	657
MW577651(8)C.C.C	657
MW579548(9)C.C.C	657
MW577652(10)C.C.C	657

Figure 11. Alignment of partial DNA sequence of the cytochrome c oxidase I from the 10 collected samples of *B. jamesi* (NCBI Acc. Nos. MW575424, MW575449, MW575455, MW580729, MW580730, MW575454, MW577650, MW577651, MW579548, MW577652 and reference sequence of *B. jamesi* KX417647.

Bathynomus kensleyi Lowry and Dempsey, 2006 was described from off the Great Barrier Reef, Queensland, with additional material from the Philippines and from ‘south of Hong Kong’. An examination of good-quality photos of the holotype of *B. kensleyi* (Figure 2) shows several distinct points of difference between *B. jamesi* and *B. kensleyi*: in *B. jamesi* the clypeus has a weakly produced median point, with lateral margins that converge towards the anterior, and the anterior margins are weakly concave (in *B. kensleyi* the median point is strongly produced, the lateral margins are parallel; the anterior margins strongly concave); in *B. jamesi* pleonite 3 laterally extends posteriorly to the posterior of pleonite 4 and does not exceed pleonites 4 and 5 (in *B. kensleyi* pleonite 3 laterally extends past both pleonites 4 and 5 and reaches the anterior of the pleotelson, and pleonite 4 also extends to just

posterior of pleonite 5); other differences include the uropodal exopod being proportionally shorter than in *B. kensleyi* and the posterior margin of the pleotelson being slightly narrower (0.9 times as wide as anterior width) than in *B. kensleyi* (1.0 times as wide as anterior width). The characters of the clypeus and pleon allow for identification of these two similar species. Lowry and Dempsey's (2006) synonymy included the record of Soong (1992) from the South China Sea. The figures given by Soong (1992) agree with *B. jamesi* with regard to the morphology of the pleon, clypeus and pleotelson, confirming that *B. kensleyi* does not occur in the South China Sea. The *Bathynomus* specimens identified as *B. kensleyi* in Lowry and Dempsey (2006) from the northern Philippines are in fact *B. jamesi*, but those from the Sulu Sea are neither *B. jamesi* nor *B. kensleyi*, and appear to be an undescribed species (see 'Discussion').

The 10 *B. jamesi* collected from Pratas Island share the common feature of a huge body size (277 to 376 mm, all specimens), with 11 upwardly curved pleotelsonic spines (Figures 3(a) and 4(a,c)). According to Lowry and Dempsey's (2006) description, only two *Bathynomus* species, *B. kensleyi* and *B. lowryi*, have these characteristic upwardly curved pleotelsonic spines. The present specimens display all the diagnostic characteristics of *B. jamesi* from Kou et al. (2017), but the pleotelsonic spines, not described in the diagnosis, are different. In Kou et al.'s (2017) specimens the pleotelson spines project straight (or perhaps just slightly angled up in lateral view), in line with the pleotelson (Kou et al. 2017), Figure 1(b), whereas in the present material they are upturned. Given that the molecular data shows that all these specimens are the same species, and in the absence of other morphological difference, we conclude that the development of pleotelson spines is an expression of age and maturity; the Kou et al. (2017) specimens are small juveniles and one small immature specimen, so adult characteristics were not assessed. *Bathynomus jamesi* is the third species of *Bathynomus* to show strongly produced and dorsally directed pleotelson spines in the mature individuals of both sexes.

The colouration of *B. lowryi* Bruce and Bussarawit, 2004 from Thailand is similar to that of the present specimens of *B. jamesi* (Figure 8(a)), except that the pleopods of *B. lowryi* are grey and dark orange, not dark rose (Bruce and Bussarawit 2004).

The presence of oostegites on the pereopods of the present females (TMCD003332) indicates that *B. jamesi* reaches maturity before attaining a body length of 277 mm.

***Bathynomus* sp.**

Material

TMCD003326 and TMCD003334

One ovigerous female, collected by bottom trawl in the northern South China Sea between North Vereker Bank (221.061°N, 116.109°E) and Pratas Island (20.717°N, 116.700°E) by the crew of Keelung-based fishing vessel *Jin Ruiyi 37* on 17 June 2019 (Figure 1) voucher numbers TMCD003326. One male, captured in waters of the South China Sea (19.084°N, 115.250°E) by the crew of Keelung-based fishing vessel *Jing yang* on 12 May 2020; the water depth was about 420–550 m, TMCD003334. TL 309 and 356 mm, CL 150 and 173 mm, wet weight 1100 and 1600 g, respectively (Table 1).

Remarks

Two apparently sympatric species of *Bathynomus* are present in the material examined. Both of these had been identified as *Bathynomus jamesi* (Kou, Chen and Li, 2017); that identification was confirmed by COI data (NCBI Acc. No. MW575424 and MW577652).

The second apparent species, while having the same clypeus and pleonite characters as *B. jamesi*, differs from *B. jamesi* s. str. in a number of significant characters (state of *B. jamesi* in parentheses): the body is slender, with the pereon lateral margins relatively straight (vs convex); the pleotelson is 0.70 times as long as wide (vs 0.42–0.56); the pleotelson spines are flat and proximally broad (vs round, proximally narrow). These morphological character differences would be considered indicative of a separate species, but at present we are unable to discern further differentiating characters. Furthermore, COI data indicates that this material is conspecific with the South China Sea material identified as *B. jamesi*. At present we regard the identity of these specimens as inconclusive, and prefer to exclude the material from *B. jamesi* until further specimens are available to either evaluate variation within *B. jamesi* or confirm that the material represents a distinct species.

Bathynomus yucatanensis sp. nov.

([urn:lsid:zoobank.org:pub:399605D3-356E-402D-9ED1-E36A649A3F1B](https://doi.org/10.21203/rs.3.rs-1234567/v1))

Material examined

Holotype. Male obtained from an aquarium as noted above (voucher number TMCD003335, NCBI Acc. No. MZ354630 for COI and MZ042927 for 16S rRNA), the TL 257 mm, CL 129 mm, and wet weight 550 g (Table 1). Reportedly caught in a baited cage at 600–800 m depth on 19 April 2017 in the Gulf of Mexico off the Yucatán Peninsula.

Diagnosis

Clypeus with straight lateral margins. Antennal flagellum extending to within pereonite 3. The distal part of the coxa of pereopod 7 is broad. Uropodal exopod not extending beyond pleotelson: endopod with distolateral corners slightly produced. Length:width ratio of pleotelson approximately 0.8:1; number of pleotelsonic spines 11 or 13, short, or straight.

Description of male (TMCD003335)

Body (Figure 13(a)) 260 mm in TL, 2.6× times longer than wide. Head ridge above eyes discontinuous (Figure 13(b)); clypeal region with distal margin distinctly concave, apex narrowly rounded (Figure 13(c)).

Flagellum of antennula longer than peduncle, more than 48 articles (lacking terminal part of both antennulae). Antenna article 1 very short, article 2 about 1.5 times longer than 1, articles 3–4 bearing neither exopod nor seta (Figure 15(h)), article 5 extremely short (Figure 15(i)); flagellum longer than peduncle, extending to within pereonite 3 (Figures 13(d) and 14(a)), composed of approximately 55 articles (near-terminal segmentation unclear).

Mandible with broad tridentate incisor. Palp extending beyond cutting edges.

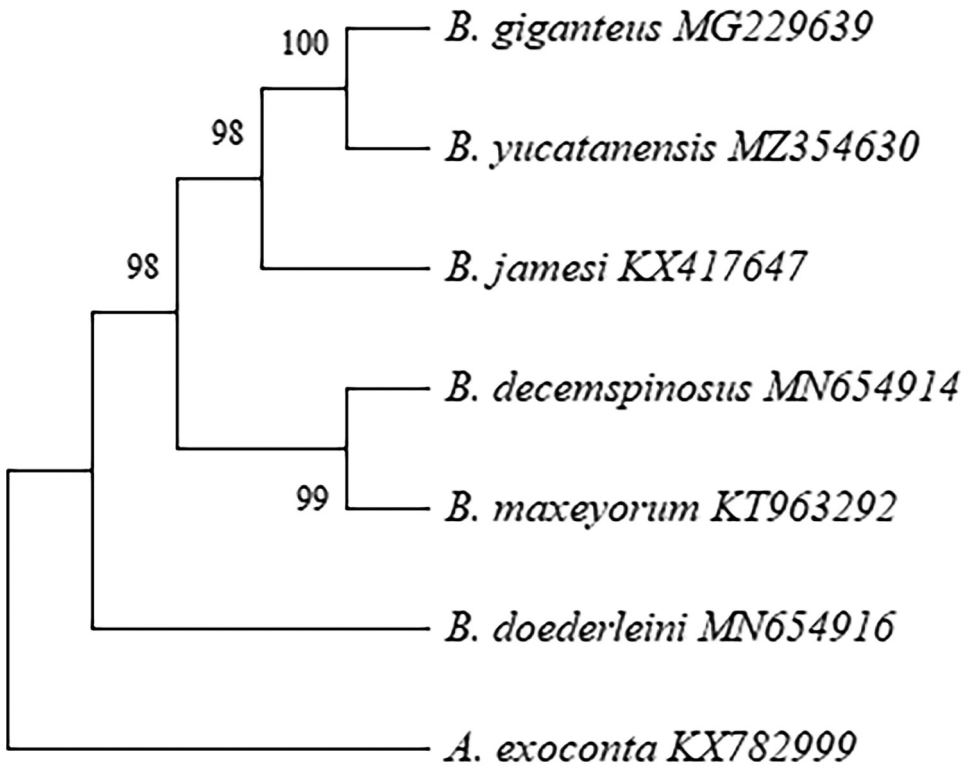


Figure 12. Phylogenetic tree based on the DNA sequences of cytochrome *c* oxidase I (COI). The sequences were aligned using Clustal Omega, and the tree was constructed by the neighbour-joining method. Numbers at branches indicate bootstrap values. The sequence of Cirolanidae (*Atarbolana exoconta*, KX782999) COI was used as the outgroup. Evolutionary analyses were conducted in MEGA 11.

Mandible palp not reaching the incisor margin (Figure 17(d)). Maxilla with long setae (Figure 17(c)); lateral lobe with 9 keratinised spines on exopod, 3 RS on endopod (Figure 17(e)). Maxillipedal palp (Figure 17(a)) with broad articles bearing plumose setae on lateral margins and simple setae on medial margins, all articles wider than their articulating junctions, and terminal article triangular; maxillipedal endite with 5 equally coupling setae (Figure 17(b)).

Pereopod 1 (Figure 15(a)) with ischium bearing 3 posteroproximal RS and 3 RS on posterodistal margin; merus bearing 3 RS on an anterodistal angle, 3 RS in a proximal row on posterolateral margin, and 3 RS in a distal row; propodus twice as long as wide, with 5 RS on posterior margin. Pereopod 2 (Figure 15(b)) with ischium bearing 3 RS each on posterior and posterodistal margins; merus with 7 short setae on an anterodistal angle, 3 RS in a proximal row along the posteromedial margin, and 3 RS in a distal row; and propodus with 5 RS on posterior margin. Pereopod 7 basis 2.5 times as long as greatest width, superior margin convex, inferior margin with 5 palmate setae; ischium 0.7 times as long as basis, inferior margin with 14 RS (4 clusters of 1 + 3 + 6 + 4), superior distal angle with 12 RS, inferior distal angle with 6 RS; merus 0.5 as long as ischium, 2.1 times as long as wide, inferior margin with 6 RS, superior distal angle with 9 RS, inferior distal angle with 8

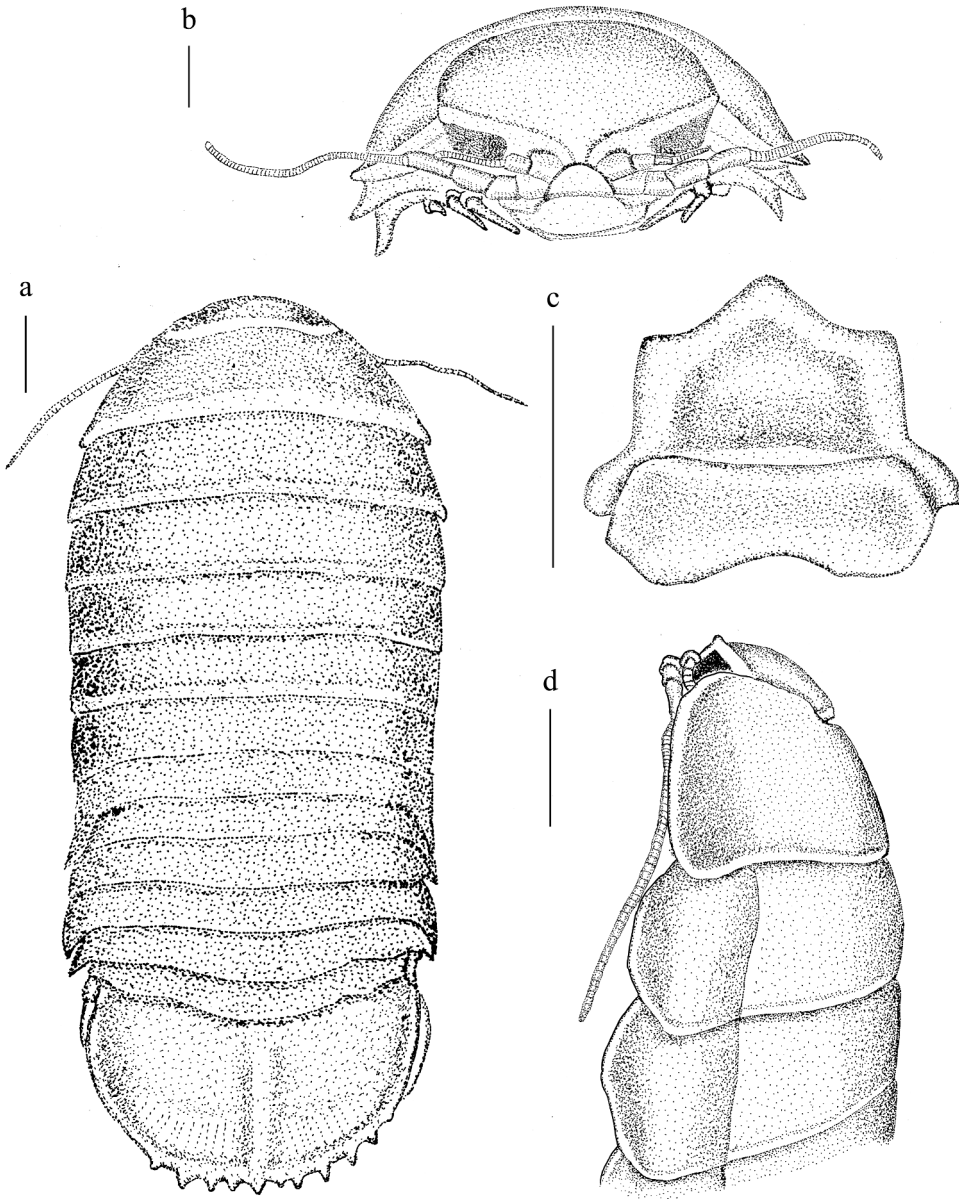


Figure 13. *Bathynomus yucatanensis* sp. nov. Holotype (voucher no. TMCD003335). (a) Body, dorsal view; (b) cephalon, anterior view; (c) clypeal region, ventral view; (d) cephalon, lateral view. Scale bars: 1 cm.

RS; carpus 0.6 times as long as ischium, 1.6 times as long as wide, inferior margin with 5 RS (as 1 + 2), superior distal angle with 13 RS, inferior distal angle with 9 RS; propodus 0.7 times as long as ischium, 2.4 times as long as wide, inferior margin with 6 clusters of RS (as 3 clusters of 2), superior distal angle with 4 slender setae, inferior distal angle with 1 RS; dactylus 0.5 times as long as propodus.

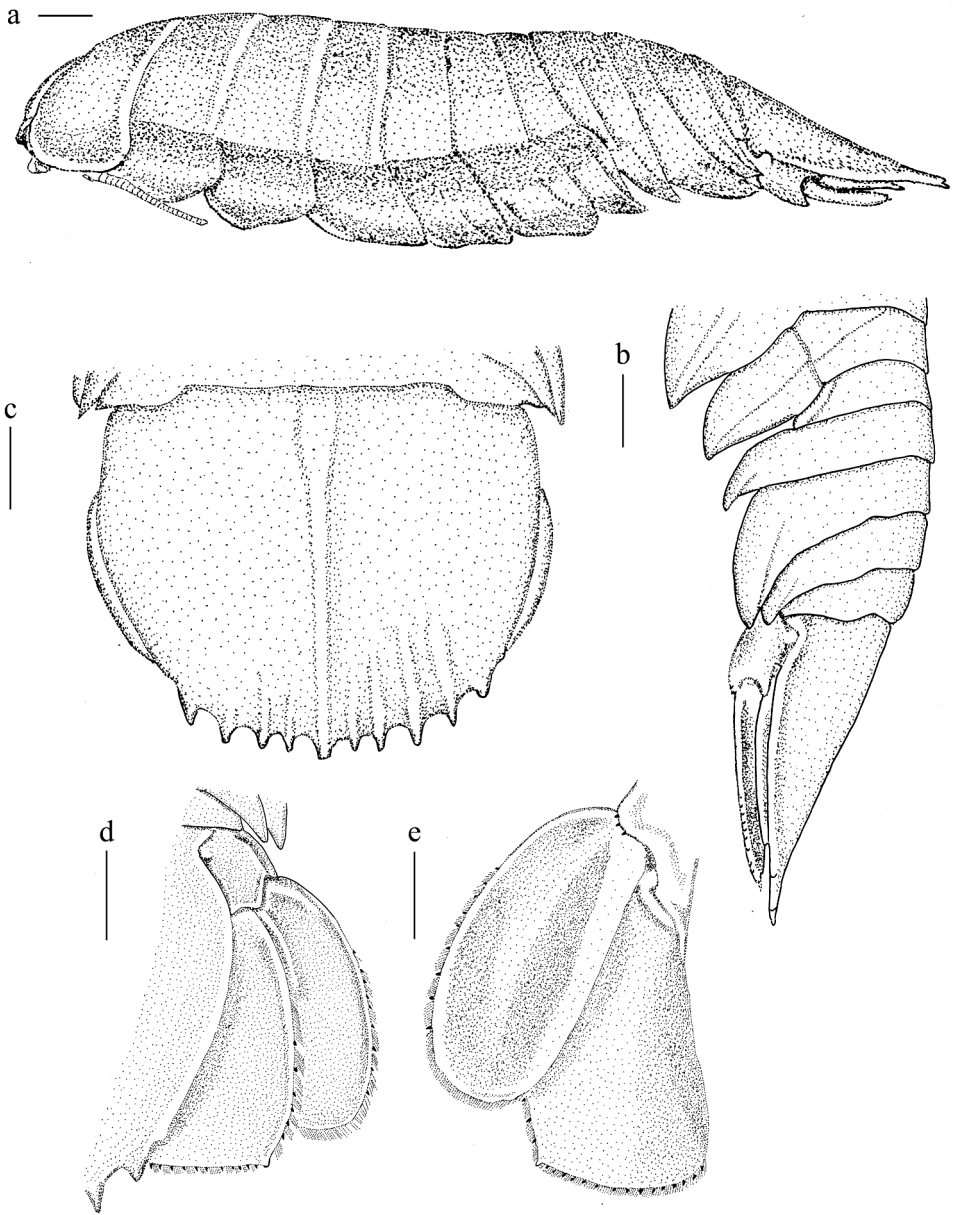


Figure 14. *Bathynomus yucatanensis* (voucher no. TMCD003335). (a) Body, lateral view; (b) pereopod, lateral view; (c) pleotelson, dorsal view; (d) uropod, dorsal view; (e) uropod, ventral view. Scale bars: 1 cm.

Coxa of pereopod 7 distally broadened and slightly upcurved posteriorly (Figures 14(a,b)).

Penial processes separated by 5% of sternal width (Figure 16(f)).

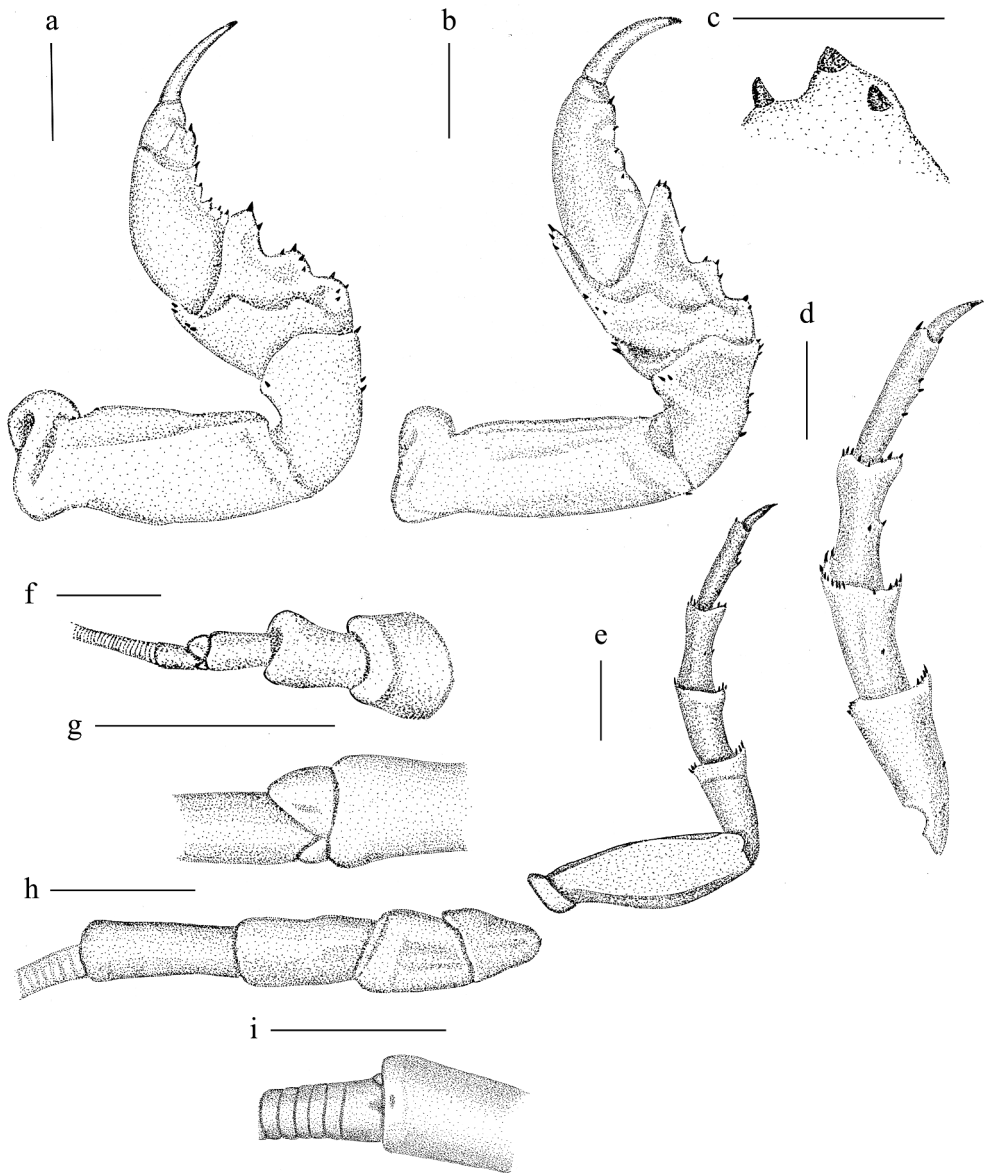


Figure 15. *Bathynomus yucatanensis* (voucher no. TMCD003335). (a) Pereopod 1, mesial view; (b) pereopod 2, mesial view; (c) pereopod 2 merus, posterolateral margin, (d, e) pereopod 7; (f) antennula; (g) antennal peduncle article 4; (h) antennal peduncle; (i) antennula peduncle article. Scale bars: 1 cm.

Pleon comprises approximately 20% of body length (Figures 13(a) and 14(a)). Posterolateral angles of pleonites 3–5 reach almost the same level posteriorly (Figure 14 (a,b)). We did not find an appendix masculina on the pleopod.

Uropods (Figure 14(c)) not extending to posterior margin of pleotelson. Peduncle ventrolateral margin with 3 ventral RS (Figure 14(e)). Exopod with smooth lateral and distal margins (Figure 14(d)); with 7 RS (Figure 14(d,e)) along the lateral margin, straight

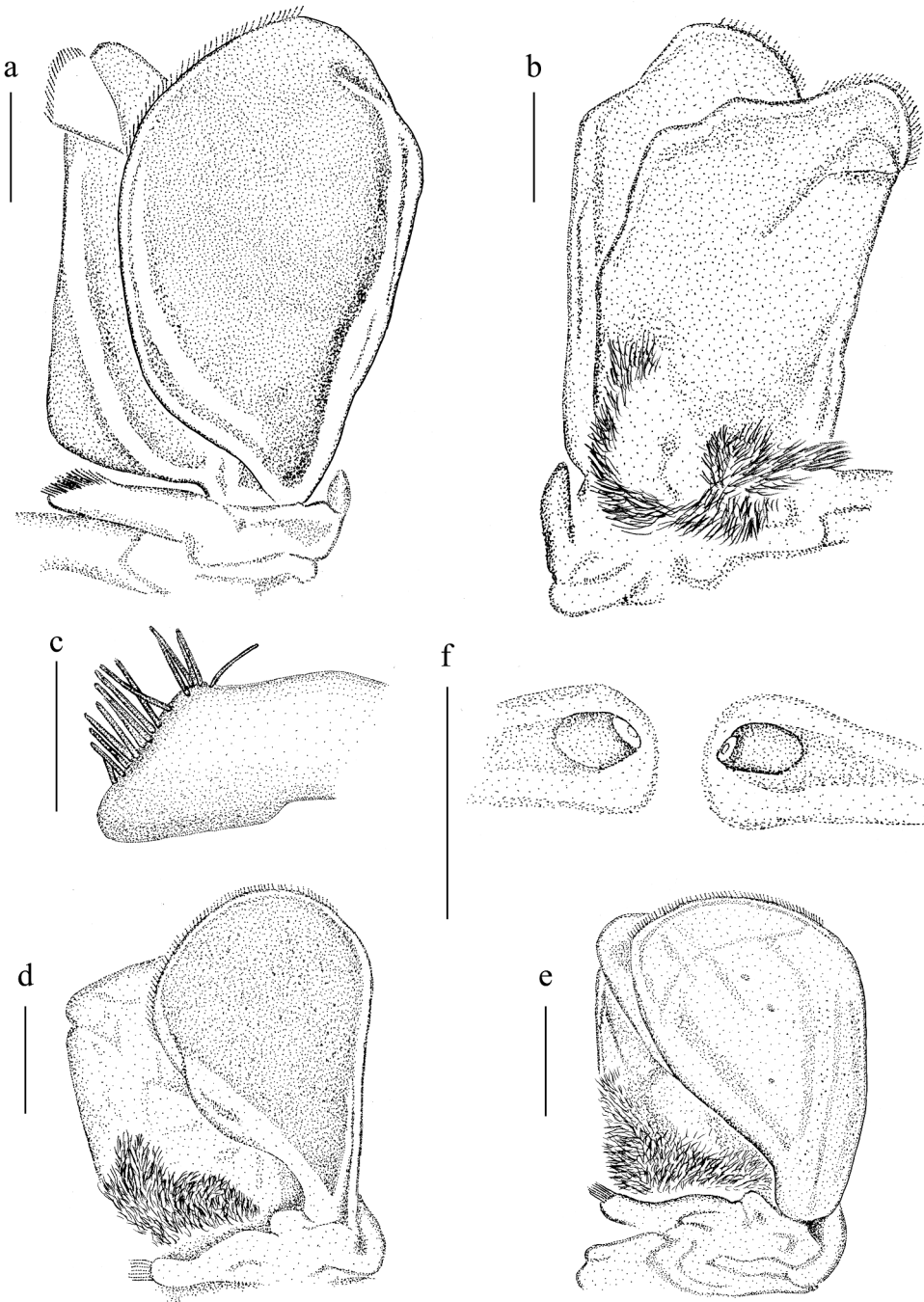


Figure 16. *Bathynomus yucatanensis* (voucher number TMCD003335). (a) pleopod 1, ventral view; (b) pleopod 1, dorsal view; (c) peduncle, ventral view; (d) pleopod 2, ventral view; (e) pleopod 3, ventral view; (f) penes, ventral view. Scale bars: a, b, d–f = 1 cm; c = 0.5 cm.

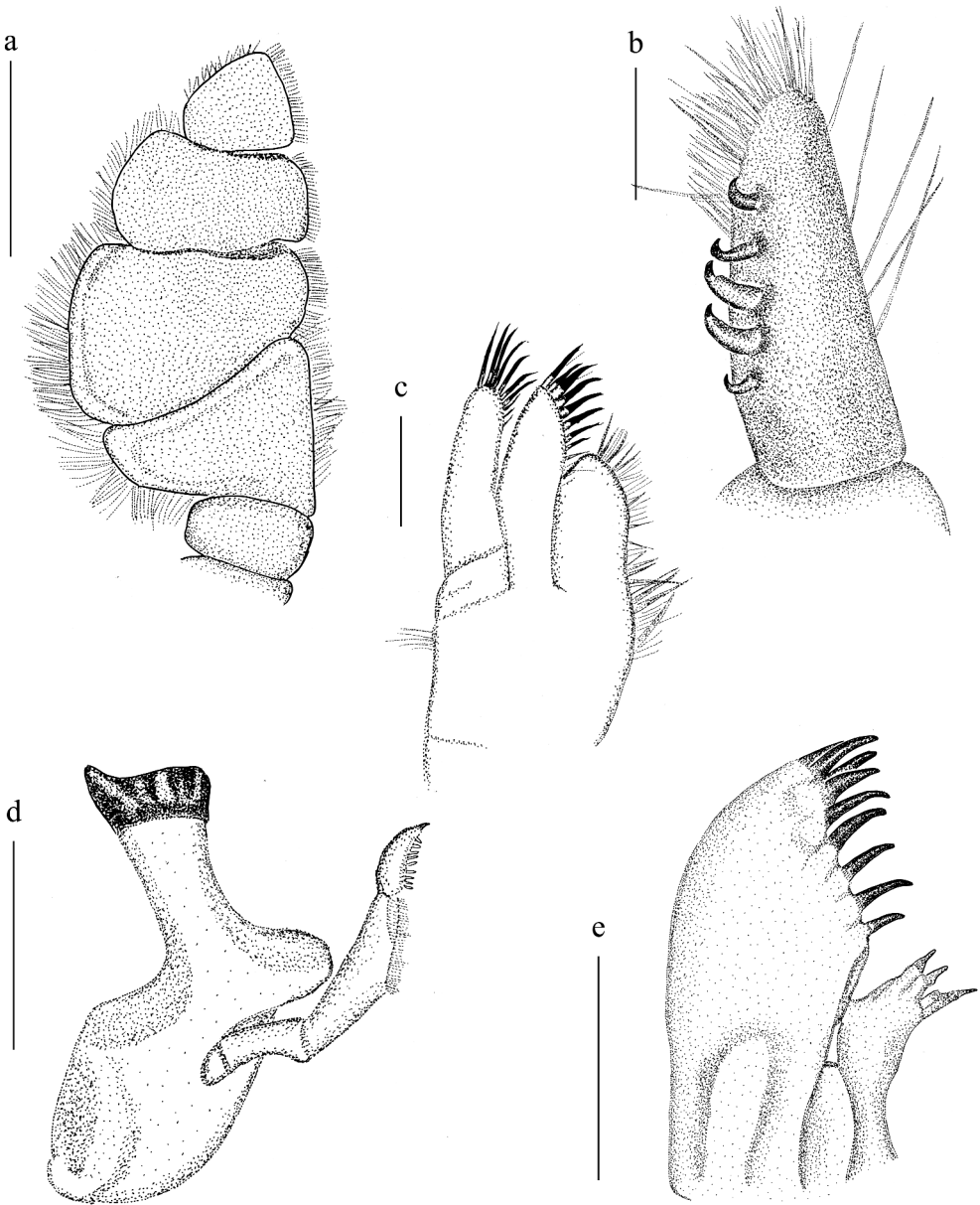


Figure 17. *Bathynomus yucatanensis* (voucher no. TMCD003335). (a) Maxillipedal palp; (b) maxillipedal endite; (c) maxilla; (d) mandible; (e) lateral lobe of maxilla. Scale bars: a, d, e = 1 cm; b, c = 2 mm.

medial margin, and distomesial corner rounded; convex distal margins both lacking setae, and distolateral corner not produced, distolateral corner subacute. Endopod (Figure 14(d, e)) lateral margin straight with 9 RS, medial margin straight, distomesial angle rounded, distal margin straight with 15 RS, distolateral angle slightly produced, subacute.

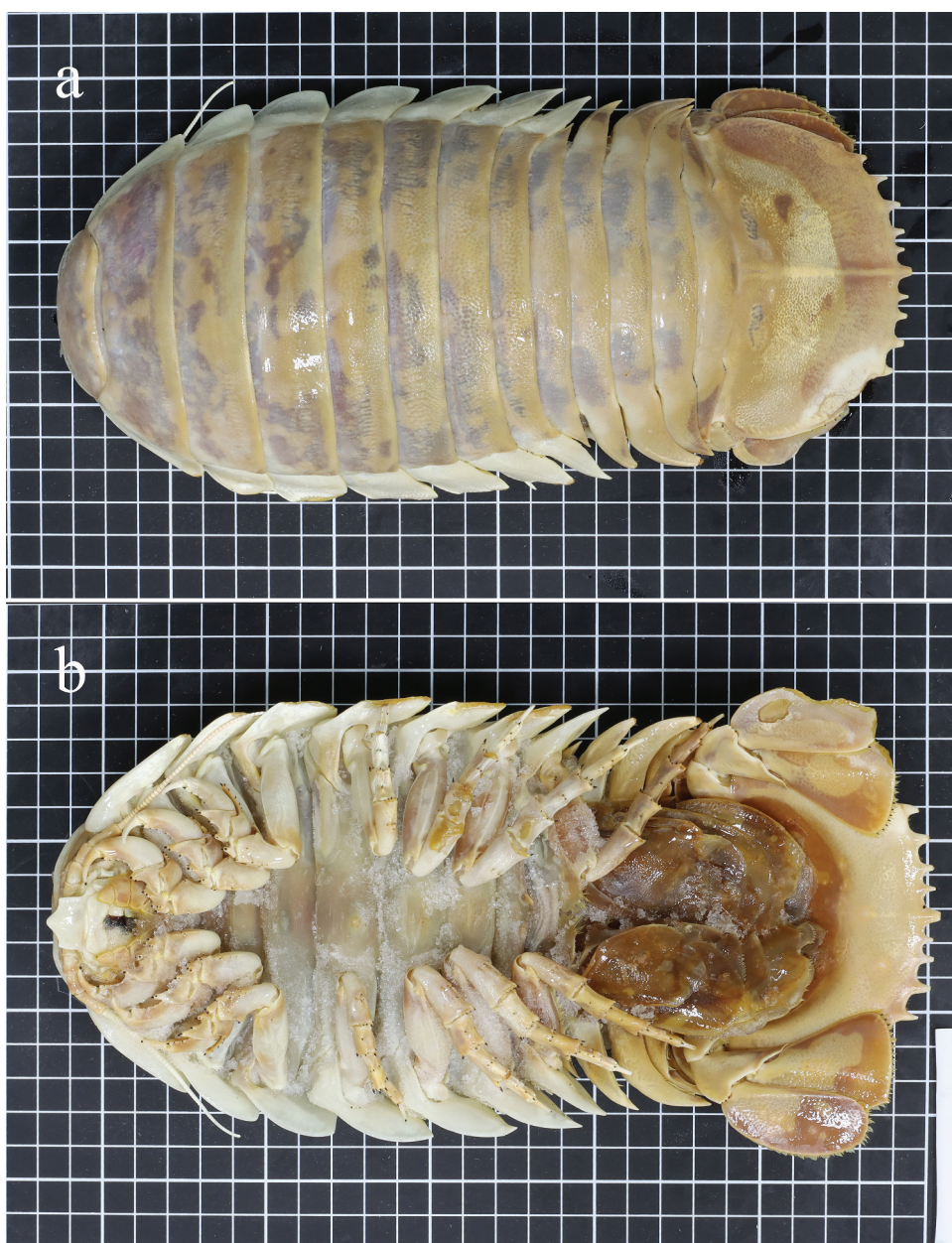


Figure 18. *Bathynomus yucatanensis* (voucher no. TMCD003335). Body length 260 mm. (a) Dorsal view; (b) ventral view. Each square is 1 cm on a side.

Pleotelson (Figure 14(b,c)) approximately 0.5 times as long as wide, smooth except for minute pores; with inconspicuous longitudinal carina on dorsal surface, running anterior from pleotelsonic spines; vestigial spines and posterior margin with 10 prominent spines and 1 pair of vestigial spines (Figure 14(c)), all long and straight with no setae between them, central distal spine simple.

35 places from that of a specimen of *B. giganteus* registered in NCBI (MG229639) (Figure 19). The alignment of 16S rRNA nucleotides among *Bathynomus* species in the Gulf of Mexico is also shown in Figure 20. COI and 16S rRNA sequencing revealed that the two individuals of *B. giganteus* were different species. After comparing them with the NCBI database, we found that one was *B. giganteus*, but the other did not correspond to any known species. Comparisons with descriptions of existing species showed that it was a new species. Due to the different sequences of the two genes (COI and 16S rRNA) (Figures 19 and 20), coupled with differences in morphology (Table 3), we identified it as a new species.

Remarks

Two *Bathynomus* species are known from the Gulf of Mexico, *B. giganteus* and the recently described *B. maxeyorum*. Compared to *B. giganteus*, *B. yucatanensis* has more slender body proportions and is shorter in total length than *B. giganteus*, and the pereopods are more slender. The antennal flagellum extends to pereonite 3 in *B. yucatanensis* vs reaching pereonite 2 in *B. giganteus*; pereonite 3 is widest (vs pereonite 5: the pereon shape of *B. yucatanensis* is an inverted triangle vs ovate in *B. giganteus* (Bruce 1986)). The pleotelson spines of *B. yucatanensis* are more slender than those of *B. giganteus*. The coxal plates in *B. yucatanensis* are pale in comparison to those of *B. giganteus*.

Compared with *B. maxeyorum*, the most distinctive feature is the number of pleotelson spines (11 spines in *B. yucatanensis* vs 7 in *B. maxeyorum*), the uropod exopod distolateral corner is not produced in *B. yucatanensis* vs produced in *B. maxeyorum*, and in *B. yucatanensis* the clypeus anterior margins are concave and the lateral margins straight vs anterior margins straight and lateral margins concave in *B. maxeyorum* (Shipley et al., 2016) (Figure 1(e)).

These morphological characters have been used as diagnostic characteristics and keys to identify and describe species (Bruce 1986; Bruce and Bussarawit 2004; Lowry and Dempsey 2006; Kou et al. 2017). The colour of the lateral margin of the pereion, width of pereopods, longitudinal median carina on pleotelson, and proximal width of the pleotelson spines clearly differ between *B. giganteus* and *B. yucatanensis* (Table 3). These morphological characters have not previously been used as diagnostic characters, but differences in these morphological features are consistent with the results of molecular analyses in the present study (Figures 10–12).

Discussion

Bathynomus jamesi vs *Bathynomus kensleyi*

Two species of 'super-giant' *Bathynomus* have been described from the northern South China Sea region; one is *B. kensleyi* and the other is *B. jamesi*. Lowry and Dempsey (2006) recorded *B. kensleyi* from south of Hong Kong (20.334°–20.834°N, 115.500°–116.250°E); their specimens clearly showed upwardly curved pleotelsonic spines, and *B. kensleyi* was the only 'super-giant' *Bathynomus* species known in the South China Sea at that time. Kou et al. (2017) described *B. jamesi* from 100 kilometres south-east of Hainan Island and

Table 3. Comparison of morphological and ecological characters between *Bathynomus yucatanensis* sp. nov. and *B. giganteus*.

Species	<i>B. yucatanensis</i> sp. nov. **	<i>B. giganteus</i>
Clypeus: lateral margins	Straight	Straight*
Antennal flagellum reaching	Pereonite 3	Pereonite 2*
Pereonites 7 (Pereonites 7/4)	Narrow (0.87)	Not narrow (1.0)**
Lateral margin of pereonites: colour	Cream yellow	White**
Pereopod 7: shape of distal part of coxa	Broad	Broad*
Appendix masculina (male)	Absent	Present**
Width of pereopod basis	2.5 as long as wide	3.2 as long as wide **
Pleotelson length: width ratio	ca. 0.5	ca. 0.5*
Longitudinal midline on pleotelson	Present	Absent**
Pleotelson spines: number	12	11–13*
Pleotelson spines: shape	Straight	Straight*
Pleotelson spine: thickness	Stout	Slender**
Uropodal endopod: distolateral corner	Slightly produced	Slightly produced*
Uropodal exopod: distolateral corner	Not produced	Not produced*
Habitat depth	c. 600–800 m	170–2140 m*
Distribution	Gulf of Mexico	West Atlantic Ocean*

*Data from Kou et al. (2017) and Table 2; **Data from present observation in Figures 18 and 21. ca.: circa.

believed that *Bathynomus* sp. from the Gulf of Aden (Lowry and Dempsey 2006) was the same species as *B. jamesi*. All of these specimens of *Bathynomus* sp. and *B. jamesi* were immature or juvenile.

The COI sequences of our 10 sample individuals of *B. jamesi* are consistent with sequences of Kou et al. (2017) (NCBI Acc. No. KX417647), confirming that they are the same species as *B. jamesi* (Figure 11). All material examined by Kou et al. (2017) was immature, and none of the individuals showed ‘upwardly curved pleotelsonic spines’. In contrast, the 10 mature individuals we collected all show the ‘upwardly curved pleotelsonic spines’ that is characteristic of *B. kensleyi*. However, as discussed in the ‘Remarks’ for *B. jamesi*, *B. kensleyi* differs noticeably from *B. jamesi* with regard to clypeus and pleon morphology, and also in the fine detail of the uropodal rami. It is clear that the mature adults of *B. jamesi* have upturned elongate pleotelson spines, and that three species now share this character: *B. jamesi* from the South China Sea; *B. kensleyi* from the Coral Sea in eastern Australia (see comments on *B. kensleyi* below); and *B. lowryi* from the Andaman Sea, Thailand.

Truong (2015) identified *Bathynomus* species found off the Spratly Islands in the South China Sea as *B. kensleyi*, with the characteristic 11 upwardly curved pleotelsonic spines, but this species shows the clypeus, pleon and uropodal characters of *B. jamesi*, and is here recognised as that species.

B. kensleyi has only one entry in NCBI (Acc. No. MN654915), from India (Prasanna Kumar et al. 2020). A comparison shows that the DNA sequence of the COI from NCBI (India sample) differs from each of the 10 individual sequences from the South China Sea. Direct comparison of the figures given by Prasanna Kumar et al. (2020) and Sankar et al. (2011) show that the specimen from India has been misidentified: it is neither *B. jamesi* nor *B. kensleyi* and may represent an undescribed species.

We used COI as the main basis for species identification, and 16S rRNA as an auxiliary mechanism for identifying the target species. As noted above, our recovered DNA sequences of *B. jamesi* for COI were not completely identical among individuals. Although the DNA sequence of COI displays individual differences, it is not

a systematic variable (Figure 11). These variations can be regarded as single nucleotide polymorphisms (SNPs). The SNPs were found at seven of 657 bp loci (Figure 11). We interpret this as an individual, not taxonomic, variation because the ratio is low (the maximum is 3/657 on TMCD003332 (NCBI Acc. No. MW577651)). The most mutable point appeared to be position 348, where A > T (in three individuals) and A > C (in two individuals) were both found. These results show that genetic diversity exists within the population, and that they have the potential to produce morphological variation and even new species.

Although the COI sequences of the 10 individuals are almost the same, there appear to be two phenotypes (Table 1). With respect to the identification of *Bathynomus* in terms of the length of the flagellum, in most specimens it extends to pereonite 2, but in a few (such as TMCD003328 and TMCD003333) it can reach pereonite 3. Eight of our specimens were stout-bodied and two were slim-bodied (Table 1 and Figure 9), the former being widest at pereonite 5 (vs pereonite 4) and having long, pointed pleotelson spines (vs stubby spines). Pleotelson length ranged from 1.51 to 2.71 times the width, with a large difference (Table 1) among all 10 specimens. Due to the apparent difference in appearance, if the slim-bodied group is separated, it may potentially be regarded as a different species, while the stout-bodied type conforms to *B. jamesi*. There are differences in the number of pleotelson spines and RS as well (Tables 1 and 4). COI and 16S rRNA sequences are reliable methods, but unfortunately, many molecular biologists are not familiar with the taxonomy of this group or how to identify its species. Incorrect identification creates many problems. The identification of *B. kensleyi* (MN654915) from the Indian Ocean is incorrect (Sankar et al. 2011), and it is improbable that *B. doederleini*, *B. kensleyi*, *B. decemspinus* (from Parangipettai, India), and *B. giganteus* (from Chennai, India) occur in the Indian Ocean (Prasanna Kumar et al. 2020) as no species of *Bathynomus* is known to have a trans-ocean distribution (Magalhães and Young 2003; Lowry and Dempsey 2006; Sidabalok et al. 2020).

The misidentification of *Bathynomus* sp. by Sankar et al. (2011) and Prasanna Kumar et al. (2020) can be seen in both the morphology and DNA sequences of COI. The morphology of *B. decemspinus* in terms of the central spine is significantly different from that of the holotype (Sankar et al. 2011, p. 114, fig. 1 vs Shih 1972, p. 43, Plate IV); and *B. doederleini*, in terms of the pleotelson morphology and the length ratio of spines on the posterior margin, is also different. The holotype of *B. doederleini* has smaller spines on both sides of the central spines, but these characters are not present in the sample of Sankar et al. (2011 p. 114, fig. 2), Ortmann (1894, p. 193, lines 4–6) or of Lowry and Dempsey (2006, p. 177, fig. 10f), Figure 10f. It is difficult to confirm or reject the identification of *B. kensleyi* by photo (Sankar et al. 2011, p. 114, fig. 3). *Bathynomus decemspinus* has no registered DNA sequence data for comparison. *Bathynomus doederleini* has the most data for comparison (eg AB851912, MZ723938, and MK953514); there are at least six recorded positions of DNA nucleotides of various types. In *B. kensleyi*, in the DNA sequence of COI (MN654915) and the data we analysed (MW575454), there are nucleotide variants in 42 positions in the DNA sequence of COI. Finally, Prasanna Kumar et al. (2020) cited old references, claiming that *B. giganteus* was collected from in-shore waters of

Table 4. Comparison of morphological characters among *Bathynomus jamesi*, *B. kensleyi*, *Bathynomus sp.*, *B. giganteus* and *B. yucatanensis* sp. nov.

Species	<i>B. jamesi</i> (Kou et al., 2017)	<i>B. kensleyi</i> (Lowry and Dempsey, 2006)	<i>Bathynomus sp.</i> (Lowry and Dempsey, 2006)	<i>B. jamesi</i> (TMCD003332)	<i>B. giganteus</i> (TMCD003336)	<i>B. yucatanensis</i> sp. nov. (TMCD003335)
Body length/width ratio	2.2	1.6–2.2	2.5	2.4	2.1	2.6
Head ridge	Discontinuous	Discontinuous	Discontinuous	Discontinuous	Discontinuous	Discontinuous
Clypeal lateral margins	Concave	Concave*	N/A	Concave	Straight	Straight
Clypea distal margins	Concave	Concave	N/A	Concave	Concave	Concave
Antenna 2	Within pereonite 3	Within pereonite 2	Within pereonite 3	Within pereonite 2	Within pereonite 2	Within pereonite 3
Pereopod 1, propodus Length/width	1.8	1.9–2.1	2	2	2	2
Exopod	Slightly produced	Slightly produced	Produced	Slightly produced	Not produced	Not produced
Distolateral corner	Subacute	Subacute or acute	Subacute	Subacute	Subacute	Subacute
Endopod	Slightly produced	Produced or not produced	Produced	Produced	Slightly produced	Slightly produced
Distolateral corner	Acute	Acute or subacute	Acute	Subacute	Subacute	Subacute
Distolateral corner	Approximately 0.75x as long as wide	Approximately 0.6x as long as wide*	Length 0.8x width	Approximately 0.6x as long as wide	Approximately 0.5x as long as wide	Approximately 0.5x as long as wide
Pleotelson	11 stout spines, 2 lateral spines smaller (13)	9 long, prominent spines, 1–2 small lateral spines (11)	11 short, prominent spines, and 2 small lateral spines (13)	11 spines and pair of small posterolateral spines (13)	11 spines and pair of small posterolateral spines (13)	10 spines and pair of vestigial spines (12)
Shape of pleotelson spines	Straight	Upwardly curved	Straight	Upwardly curved	Straight	Straight
Central spine	Not bifid	Simple	N/A	Simple	Simple	Simple

*Data from Kou et al. (2017).

Chennai, India. Because DNA analysis is a very precise method of species identification, once the species is misidentified and submitted into the database, it can have very serious consequences.

Bathynomus kensleyi (Lowry and Dempsey, 2006) was described from off the Great Barrier Reef, in the western Coral Sea. The type locality is 'South-east of Swain Reefs, 22.918°S 154.354°E, Coral Sea, 590–606 m depth'. Additional locations in eastern Australia included off Flynn Reef and Lihou Reef (see Material examined) in the northern Great Barrier Reef. The species was also recorded from Taiwan, south of Hong Kong and the Philippines. The records from off Hong Kong and Taiwan and the specimens from Luzon, northern Philippines, have here been re-identified as *B. jamesi*. The two specimens of *B. kensleyi* from the Sulu Sea (AM P42711, P42712) differ from the holotype and other specimens from eastern Australia by a distinctly ovate pereon; deeply incised maxillipedal somite (in dorsal view); pleotelson spines fine, more 'needle-like'; pleon short, only 17% of total body length (compared to *B. jamesi* at 29%); pleonite 3 does not posteriorly overlap pleonites 4 and 5, and pleonite 4 does not extend posterior to pleonite 5; and uropodal exopod lateral margin strongly convex. The Sulu Sea specimens are also taken from a far greater depth than most *Bathynomus*, from the continental rise at 2500 metres. The Sulu Sea specimens represent an undescribed species of *Bathynomus*. At present we regard *B. kensleyi* as occurring only in the western Coral Sea; the species is not present in the South China Sea or anywhere in the Northern Hemisphere.

***Bathynomus yucatanensis* sp. nov**

At least 35 DNA residues in the COI sequence (Figure 19) of the specimen of supposed *B. giganteus* from the Gulf of Mexico that we obtained for morphological comparison with *B. yucatanensis* were different from those of a specimen of *B. giganteus* registered in NCBI (Acc. No. MG229639), strongly indicative that this material is not conspecific with *B. giganteus*.

Morphological comparison between *B. yucatanensis* and *B. giganteus* (Table 3) shows that they have about the same number of pleotelson spines; *B. maxeyorum* has considerably fewer. This suggests that superficial examination, using only pleotelson spines, could easily result in specimens of *B. yucatanensis* being misidentified as *B. giganteus*. *Bathynomus giganteus* was discovered over a century ago, and more than 1000 specimens have been studied (1651 samples) (Briones-Fourzán and Lozano-Alvarez 1991) with no suggestion until now of a second species with the same number of pleotelsonic spines. Using the number or percentage of non-identical nucleotides alone as an indication of species boundaries would be both arbitrary and subject to error (Meier et al. 2022). However, molecular data may be an indication that additional morphological studies are needed to confirm that taxonomic separation of species is warranted.

The morphology and position of robust setae on pereopods 1 and 2 are roughly the same, symmetrical and similar in number, but there are a few differences. The number of robust setae may be affected by age, moulting status and environment, so individual variation is large. Lowry and Dempsey (2006) suggest that pereopodal robust setae alone cannot serve as the basis for species identification, but the

Table 5. Comparison of number of robst setae among *Bathynomus jamesi*, *B. kensleyi*, *Bathynomus sp.*, *B. giganteus* and *B. yucatanensis sp. nov.*

Species	<i>B. jamesi</i> (Kou et al., 2017)	<i>B. kensleyi</i> (Lowry and Dempsey, 2006)	<i>Bathynomus sp.</i> (Lowry and Dempsey 2006)	<i>B. jamei</i> (TMCD003332)	<i>B. giganteus</i> (TMCD003336)	<i>B. yucatanensis sp. nov.</i> (TMCD003335)
Pereopod 1, ischium	4	1-4	4	3	5	3
Posteroproximal						
Posterodistal margin	3	2-4	5	3	3	3
Pereopod 1, merus						
Anterodistal angle	5	2-4	9	3	9	3
Poster margin, proximal row	4	4	4	3	4-5	3
Distal row	4	3-4	5	3	4	3
Pereopod 1, propodus						
Posterior margin	5	4-5	5	4	7	5
Pereopod 2, ischium						
Posterior margin	3	3-4	6	3	4-5	3
Posterodistal	3	2-3	5	3	2	3
Pereopod 2, merus						
Anterodistal angle	8	5-7	11	5	9-10	7
Posteromedial margin, proximal row	3	3-4	3	3	3	3
Distal row	3	3	4	3	4	3
Pereopod 2, propodus						
Posterior margin	3	4	4	4	5	5
Uropod, peduncle	3	2-3	2	2	6	3
Exopod						
Lateral margin	11	9	7-8	9	8	7
Distal margin	7	4-5	5	4	7	0
Endopod						
Lateral margin sinuate	5	3-6	5	3	6	9
Distal margin	9	10-13	12	10	10-11	15



Figure 21. *Bathynomus giganteus* (voucher number TMCD003336). Body length 316 mm. (a) Dorsal view; (b) ventral view. Each square is 1 cm on a side.

number of robust setae in the same species is close, and thus can still be used as a reference for identification (Table 5). In addition, the shape and colour of the male penes can also confirm species identity.

In the present instance, despite the large number of DNA nucleotide differences, which clearly refutes the possibility of conspecificity, MEGA 11 showed that *B. giganteus* is indeed the species closest to *B. yucatanensis* (Figure 12). This indicates that the two species likely had a common ancestor. Additionally, there may also be other undiscovered *Bathynomus* spp. in the tropical western Atlantic.

COI is commonly used for species identification and is the basis for DNA barcoding of many animals (Lobo et al. 2013); most species of *Bathynomus* have a COI sequence registered in the NCBI data bank. The 16S rRNA is another commonly used biomarker (Vences et al. 2005), and a few sequences of this gene have been recorded for *Bathynomus* spp. in recent years.

Relevance to fisheries

Some species of *Bathynomus* with commercial potential have become the targets of deep-sea trawl fisheries. Besides the very localised use in restaurants in Taiwan mentioned above, in Japan *B. doederleini* is made into 'sembei' rice crackers (Talwar et al. 2016) with a shrimp- or crab-like aftertaste. For the management of *Bathynomus* fisheries, it is important to know precisely which species are being caught. There may as yet be no commercial use of western Atlantic *B. giganteus*, but the likelihood of *B. yucatanensis* being confused with it is high, at least as long as the true range of the latter, and the relative proportions of both species in areas of sympatry, remain unknown.

Conclusions

We confirm the identity of *Bathynomus jamesi* in Taiwanese waters (vicinity of Pratas Island), while rejecting the occurrence of *B. kensleyi* in the South China Sea. Although there is some morphological variation in the specimens with respect to the original description, this is shown to be due to ontogenic development, with the original material being immature and juvenile; the conspecificity of all specimens was confirmed by COI and 16S rRNA sequences.

Examination of specimens and photographs of *Bathynomus kensleyi* reveals that this species is restricted to the continental slope off the Great Barrier Reef, Australia; the species does not occur in the Northern Hemisphere.

Furthermore, after analysing COI and 16S rRNA, we found that specimens of *Bathynomus* from off the Yucatán Peninsula in the Gulf of Mexico were not *B. giganteus* as expected, leading us to describe them as *B. yucatanensis* sp. nov. It is increasingly evident that species of *Bathynomus* may be exceedingly similar in overall appearance, and also that there is a long history of misidentification of species in the genus (see Lowry and Dempsey 2006; Sidabalok et al. 2020). While careful recording of morphological characters will identify species, the use of molecular biological techniques will prove valuable in confirming species identity, particularly in the case of morphologically similar species.

Acknowledgements

The authors thank Ms Fang Yi Lee, National University of Tainan, for her technical support, and also Dr Mark J. Grygier, National Taiwan Ocean University, and Dr Yukio Hanamura of the Crustacean Society of Japan for providing invaluable scientific advice and English revision after reading drafts of the manuscript. We thank Michitaka Shimomura, Field Science Education and Research Center, Kyoto University, for his comments on an early draft. MCH also thanks the owners of the seafood shop Shi Shang Xian for allowing him to inspect their wares. We express our great thanks to Gavin Dally (Northern Territory Museum and Art Gallery, Darwin), Dr S.J. Keable and Dr Laetitia Gunton (Australian Museum, Sydney) and Dr Laure Corbari and Paula Martin-Lefèvre (Crustacea collection, Muséum National d'Histoire Naturelle, Paris), all of whom very efficiently provided excellent photographs of *Bathynomus* from their collections. This work and the new species name have been registered with ZooBank under urn:lsid:zoobank.org:pub:399605D3-356E-402D-9ED1-E36A649A3F1B. This is contribution number 643 from the North-West University–Water Research Group.

Disclosure statement

No potential conflict of interest was reported by the authors.

Funding

The authors reported there is no funding associated with the work featured in this article.

ORCID

Ming-Chih Huang  <http://orcid.org/0000-0001-9237-8593>

Tadashi Kawai  <http://orcid.org/0000-0001-5988-0493>

Niel L. Bruce  <http://orcid.org/0000-0003-4745-5048>

Authors' contributions

MCH designed the study and performed the laboratory analyses. TK was responsible for morphological observations and comparison, and for the drawings. NLB was responsible for taxonomic and nomenclatural interpretation and decisions. All authors approved the final manuscript.

References

- Briones-Fourzán P, Lozano-Alvarez E. 1991. Aspects of the biology of the giant isopod *Bathynomus giganteus* A. Milne Edwards, 1879 (Flabellifera: Cirolanidae), off the Yucatan Peninsula. *J Crustacean Biol.* 11(3):375–385. doi:10.2307/1548464
- Bruce NL. 1986. Cirolanidae (Crustacea: Isopoda) of Australia. *Rec Aust Mus Suppl.* 6:1–239. doi:10.3853/j.0812-7387.6.1986.98
- Bruce NL, Javed W. 1987. A new genus and two new species of cirolanid isopod Crustacea from the northern Indian Ocean. *J Nat Hist.* 21(6):1451–1460. doi:10.1080/00222938700770911.
- Bruce NL, Bussarawit S. 2004. *Bathynomus lowryi* sp. nov. (Crustacea: Isopoda: Cirolanidae), the first record of the 'giant' marine isopod genus, from Thailand waters. *Phuket Mar Biol Cent Res Bull.* 65:1–8.
- Bruce NL. 2009. The marine fauna of New Zealand: Isopoda, Aegidae (Crustacea). Wellington: NIWA Biodiversity Memoir. 122:1–252.
- Folmer O, Black M, Hoeh W, Lutz R, Vrijenhoek R. 1994. DNA primers for amplification of mitochondrial cytochrome c oxidase subunit I from diverse metazoan invertebrates. *Mol Mar Biol Biotechnol.* 3:294–299.
- Holthuis LB, Mikulka WR. 1972. Biological results of the University of Miami deep-sea expeditions. 91. Notes on the deep-sea isopods of the genus *Bathynomus* A. Milne Edwards, 1879. *Bull Mar Sci.* 22(3):575–591.
- Keable SJ. 2006. Taxonomic revision of *Natatolana* (Crustacea: Isopoda: Cirolanidae). *Rec Aust Mus.* 58(2):133–244. doi:10.3853/j.0067-1975.58.2006.1469
- Kensley B, Schotte M. 1989. Guide to the marine isopod crustaceans of the Caribbean. Washington (DC): Smithsonian Institution Press; p. 308.
- Kou Q, Chen J, X L, He L, Wang Y. 2017. A new species of the giant deep-sea isopod genus *Bathynomus* (Crustacea, Isopoda, Cirolanidae) from Hainan Island, South China Sea. *Integr Zool.* 12(4):283–291. doi:10.1111/1749-4877.12256
- Lobo J, Costa PM, Teixeira MA, Ferreira MS, Costa MH, Costa FO. 2013. Enhanced primers for amplification of DNA barcodes from a broad range of marine metazoans. *BMC Ecol.* 13(1):34. doi:10.1186/1472-6785-13-34
- Lowry JK, Dempsey K. 2006. The giant deep-sea scavenger genus *Bathynomus* (Crustacea, Isopoda, Cirolanidae) in the Indo-West Pacific. In: Richer de Forges B, Justine J-L, editors. *Resultats des Campagnes Musortom, Tropical Deep-Sea Benthos, Mém Mus Natl Hist Nat.* Paris: Memoires du Museum National d'Histoire Naturelle, Vol. 24. Paris: Publications Scientifiques du Muséum; p. 163–192.

- Magalhães N, Young PS. 2003. *Bathynomus* A. Milne Edwards, 1879 (Isopoda, Cirolanidae) from the Brazilian coast, with description of a new species. *Arquivos do Museu Nacional Rio de Janeiro*. 61(4):221–239.
- Meier R, Blaimer B, Buneaventura E, Hartop E, von Rintelen T, Srivathsan A, Yeo D, Meier R. 2022. A re-analysis of the data in Sharkey et al.'s (2021) minimalist revision reveals that BINs do not deserve names, but BOLD systems needs a stronger commitment to open science. *Cladistics*. 38(2): 264–275. doi:10.1111/cla.12489
- Milne-Edwards A. 1879. Sur un Isopode gigantesque des grandes profondeurs de la mer. *C R Hebd Séances Acad Sci Paris*. 83:21–23.
- Milne-Edwards A, Bouvier EL. 1902. Reports on the results of dredging under the supervision of Alexander Agassiz, in the Gulf of Mexico (1877–78), in the Caribbean Sea (1878–79), and along the Atlantic coast of the United States (1880), by the U.S. Coast Survey Steamer “Blake”, Lieut.-Com. C. D. Sigsbee, U.S.N., and Commander J.R. Bartlett, U.S.N., commanding. XL. Les Bathynomes. *Mem Mus Comp Zool Harv*. 27(2):141–158, pls. 1–6.
- Nei M, Kumar S. 2000. Molecular evolution and phyogenetics. New York: Oxford University Press.
- Ortmann A. 1894. A new species of the isopod-genus *Bathynomus*. *Proc Natl Acad Sci USA (Philadelphia)*. 1894:191–193.
- Palumbi SR, Martin A, Romano S, McMillan WO, Stice L, Grabowski G. 1991. The simple fool's guide to PCR. A collection of PCR protocols, version 2. Honolulu (USA): University of Hawaii.
- Prasanna Kumar C, Rethinavelu S, Sadaipappan B. 2020. First barcodes of *Bathynomus kensleyi* (Lowry and Dempsey, 2006) and *Bathynomus decemspinus* (Shih, 1972) from the Southeast coast of India. *Reg Stud Mar Sci*. 40:101489. doi:10.1016/j.rsma.2020.101489
- Sankar R, Rajkumar M, Sun J, Gopalakrishnan A, Vasanthan TM, Ananthan G, Trilles JP. 2011. First record of three giant marine bathynomids (Crustacea, Isopoda, Cirolanidae) from India. *Acta Oceanol Sin*. 30(1):113–117. doi:10.1007/s13131-011-0097-4
- Shih CT. 1972. Note on the giant isopod genus *Bathynomus* Milne Edwards, 1879 with description of a new species. *Publ Seto Mar Biol Lab*. 21(1):31–42. doi:10.5134/175798
- Shiple ON, Bruce NL, Violich M, Baco A, Morgan N, Rawlins S, Brooks EJ. 2016. A new species of *Bathynomus* Milne Edwards, 1879 (Isopoda: Cirolanidae) from the Bahamas, Western Atlantic. *Zootaxa*. 4147(1):82–88. doi:10.11646/zootaxa.4147.1.6
- Sidabalok CM, Wong HPS, Ng PK. 2020. Description of the supergiant isopod *Bathynomus raksasa* sp. nov.(Crustacea, Isopoda, Cirolanidae) from southern Java, the first record of the genus from Indonesia. *ZooKeys*. 947:39–52. doi:10.3897/zookeys.947.53906
- Soong K. 1992. Occurrence of the giant isopod *Bathynomus giganteus* A. Milne Edwards, 1879 (Isopoda Flabellifera, Cirolanidae) in the West Pacific. *Crustaceana*. 63:291–295. doi:10.1163/156854092X00433
- Soong K, Mok HK. 1994. Size and maturity stage observations of the deep-sea isopod *Bathynomus doederleini* Ortmann, 1894 (Flabellifera: Cirolanidae), in eastern Taiwan. *J Crustacean Biol*. 14(1):72–79. doi:10.2307/1549056
- Talwar B, Brooks EJ, Dean Grubbs R. 2016. An assessment of post-release mortality for a commonly discarded deep-sea isopod (*Bathynomus giganteus*) using reflex impairment. *ICES J Mar Sci*. 73(9):2356–2363. doi:10.1093/icesjms/fsw087
- Tamura K, Stecher G, Kumar S, Battistuzzi FU. 2021. MEGA11: molecular evolutionary genetics analysis version 11. *Mol Biol Evol*. 38(7):3022–3027. doi:10.1093/molbev/msab120
- Timm LE, Moahamed B, Churchill DA, Bracken-Grissom HD. 2018. *Bathynomus giganteus* (Isopoda: Cirolanidae) and the canyon: a population genetics assessment of De Soto Canyon as a glacial refugium for the giant deep-sea isopod. *Hydrobiologia*. 825(1):211–225. doi:10.1007/s10750-018-3563-6
- Truong SHT. 2015. The first record of *Bathynomus kensleyi* Lowry and Dempsey, 2006 (Crustacea, Isopoda) in Vietnamese seawaters. *Anthol Mar Stud*. 21(1):80–83.
- Vences M, Thomas M, Van der Meijden A, Chiari Y, Vieites DR. 2005. Comparative performance of the 16S rRNA gene in DNA barcoding of amphibians. *Front Zool*. 2(1):1–12. doi:10.1186/1742-9994-2-5